W-Pos465

PROTEIN EVOLUTION ON A FOLDABILITY-FITNESS LANDSCAPE.
((**S. Govindarajan** and R. A. Goldstein)) Department of Chemistry and Biophysics Research Division , University of Michigan, Ann Arbor, MI 48109-1055, USA

Evolution determines the shape and function of the biological macromolecules. Understanding the process of molecular evolution can provide insight into the structure and function of these macromolecules and the properties of these molecules will in turn throw light on the process of evolution. We model protein evolution as a random walk in a multidimensional fitness landscape, the configuartion space representing all the possible protein sequences. The fitness of any sequence corresponds to the foldabilty of that sequence to the native state. Foldability being a universal requirement for biological proteins, such a foldability based fitness landscape approach will relate the features of protein structures and evolution. Evolutionary pressure in the form of a minimum foldability requirement was explicitly considered. We observe a phase transition to a slower non self-averaging dynamics in the landscape when the evolutionary pressure is increased. At higher evolutionary pressure sequences tend to evolve along neutral networks stretching across the sequence space, representing particular structures.

W-Pos466

MODELING PROTEIN FOLDING AS DIFFUSION ON ENERGY LANDSCAPES
((**T.-L. Chiu** and R. A. Goldstein)) Department of Chemistry and Biophysics Research Division , University of Michigan, Ann Arbor, MI 48109-1055, USA

The mechanism by which proteins fold into their native three-dimensional structures remains one of the central unsolved problems of molecular biology. Protein folding process is characterized by large *ensembles* of states, whose components depend upon external conditions. In order to approach such a process, recent theoretical work has developed a statistical characterization of the energy landscape of folded proteins. In the present study, we consider folding as diffusion on the energy landscape and use the diffusion equation to study the impact of the nature of the interactions on the folding dynamics. We focus our attention on the relationship between the specific interactions necessary for folding into the native state relative to the average strength of the interactions that result in compaction. The energy landscape is characterized by two different order parameters, one representing the degree of compactness, the other a measure of the progress towards the folded state. We first construct a one-dimensional reaction coordinate through the two-dimensional order-parameter space, compute the free-energy and effective diffusion constant for motion along this reaction coordinate, and then model the folding as diffusion along this coordinate. We find that the optimal average interaction is rather large relative to the distribution of specific interactions, meaning that under optimal conditions proteins would contract quickly and search for their native state from among the compact states.

W-Pos467

FURTHER OBSERVATIONS ON TOTAL HEIGHT/UMBILICAL HEIGHT (H/U): THE GOLDEN MEAN AND FIBONACCI SERIES.
((R.P. Spencer)) University of Connecticut Health Center, Farmington, CT 06030.

As part of a study of osteoporosis in women, we also measured H/U in order to compare the present female population with reported classical Greek measurements. The "Golden mean" dervived from the attempt to divide a line of unit length so that the ratio of the longer segment (L) to the whole line was the same as that of the shorter segment (1 - L) to the longer. Hence L = (1 - L)/L. This solves as the quadratic $(-1 +/- \sqrt{5})/2$, or L = 0.618.. The value of the entire length divided by the longer segment was 1/0.618, or 1.618. The Greek observation was that their H/U was 1.618 or Golden mean. This number is also of interest as it is the ratio in the Fibonacci series (number/preceding number). The Fibonacci series has also been used to describe the growth of certain shelled animals. The value of 1.618 also appears in Chaos theory (Chirikov,B.V.: Chaos, Solitons and Fractals 1:79, 1991). Our study encompassed women without a loss of height, as well as those with a loss of 2 cm or more from osteoporotic collapse (Clin. Nucl. Med. 14:231, 1989). Our population values of H/U ranged from 1.57 to 1.86. "Bending over" or hyperkyphosis of vertebral fractures would decrease H with little change in U, lowering the value of H/U. The present population, likely older and more obese than the ancient Greeks (and probably taller) may have a more mobile umbilicus. More fixed sites, such as the iliac bone height, should likely be utilized.

W-Pos468

A MATHEMATICAL MODEL OF THE CRUSTACEAN STRETCH RECEPTOR.
((**B. Rydqvist** and C. Swerup)). Department of Physiology and Pharmacology, Karolinska institutet, S-171 77 Stockholm, Sweden.

Systems analysis has been applied for the investigation of the input-output relations of the crayfish stretch receptor, a mechanoreceptor analogous to the human muscle spindle. This type of analysis results in mathematical models consisting of a black box with input-output properties similar to the stretch receptor. With increasing knowledge, however, it has become possible to simulate each step in the transduction process between mechanical stimulation and electrical response and in this way create a composite model which gives insight into the transformation at the different stages.
In the present study a mathematical model has been developed of the transduction process in this mechanoreceptor, taking into account the viscoelastic properties of the accessory structures of the receptor (i.e. the receptor muscle), the biophysical properties of the mechanosensitive channels, the passive electrical properties of the neuronal membrane (leak conductance and capacitative properties) and voltage gated ion channels generating impulses. The parameters of the model are derived from studies on the mechanical properties of the receptor muscle, experiments on whole cell recordings of the sensory neuron and from single channel studies of the mechanosensitive channels. The viscoelastic properties of the receptor muscle are modelled by a Voigt element (spring in parallel with a dashpot) in series with a nonlinear spring. The receptor current at different extensions of the receptor was computed using typical viscoelastic parameters for a receptor muscle together with a transformation of tension in the muscle to tension in the neuronal dendrites and finally taking into account the properties of the mechanosensitive channels. The receptor potential was calculated by modelling the neuronal membrane by a lumped leak conductance and capacitance. For the calculation of potential the cell was treated as an idealized spherical body. Voltage gated ion channels were modeled using Hodgkin-Huxley formalism. The model resulted in nonlinear differential equations which were solved by an iterative, fourth order Runge-Kutta method. The performance of the model was greatly improved by introducing an intrinsic adaptation of the mechanosensitive channels. The model can predict a wide range of experimental data from the stretch receptor neurons including the mechanical response of the receptor muscle, the receptor current and its voltage dependence, the receptor potential and the impulse response.

REGULATION OF ION CHANNELS BY HETEROTRIMERIC G PROTEINS

Th-AM-SymI-1 **D. Lambright, University of Massachusetts**
Structural Determinants of G Protein Coupled Signaling

Th-AM-SymI-2 **S. Ikeda, Medical College of Georgia**
Role of G-βγ Subunits in Neuronal Calcium Channel Regulation

Th-AM-SymI-3 **G. Szabo, University of Virginia**
Functional Implications of G Protein Regulated Channel Kinetics

Th-AM-SymI-4 **D. Clapham, Harvard Medical School**
G Protein Gated K^+ Channels

Th-AM-A1

INTERACTIONS OF STRUCTURAL C DOMAIN AND REGULATORY N DOMAINS OF TROPONIN C WITH REPEATED SEQUENCE MOTIFS IN TROPONIN I. ((J.R. Pearlstone, B.D. Sykes and **L.B. Smillie**)) MRC Group in Protein Structure & Function, Department of Biochemistry, University of Alberta, Edmonton, Canada T6J 2B3.

The actomyosin ATPase inhibitory protein Troponin I (TnI) through its calcium dependent interactions with Troponin C (TnC) and actin plays a central regulatory role in skeletal and cardiac muscle contraction and relaxation. Employing single Trp mutants of TnC and its isolated structural C and regulatory N domains, curve-fitting analyses of fluorescence changes induced by increasing TnI fragment concentration have yielded dissociation constants K_{D1} and K_{D2} for the interaction of TnI_{96-116}, TnI_{96-148} and $TnI_{117-148}$ with the C and N domains, respectively, of intact TnC in its calcium saturated state. The data demonstrate that TnI residues 96-116 are largely responsible for binding to C domain and residues 117-148 to N domain. Inspection of the available mammalian and avian skeletal fast and slow muscle TnI amino acid sequences reveals a common structural motif repeated three-fold, once in the inhibitory peptide region (~residues 101-114; designated α) and twice (β and γ) in the region of residues ~121-132 and ~135-146. The number and distribution of these motifs have important structural implications for the TnI•C complex. In the β motif of cardiac TnI, as compared with skeletal, several charged amino acid changes are suggested as candidates responsible for the greater sensitivity of cardiac Ca^{2+} regulated actomyosin to acidic pH as in ischemia. (Supported by Medical Research Council of Canada.)

Th-AM-A2

NMR STUDIES OF DRUG BINDING TO CARDIAC TnC AND THE RELATIONSHIP TO THE SOLUTION STRUCTURE OF CARDIAC TnC. ((Quinn Kleerekoper*, Wen Liu*, Sam Sia#, Monica Li#, Leo Spyacopalous#, Stephane Gagne#, Brian Sykes#, and John A. Putkey*)) Department of Biochemistry and Molecular Biology, Univ. of Texas Med. School, Houston, TX, 77030 and Department of Biochemistry, University of Alberta, Edmonton, Canada.

The ability of drugs, such as bepridil and trifluoperazine (TFP), to bind to cardiac troponin C (cTnC) and increase the affinity of its regulatory Ca^{2+}-binding site, has prompted a search for Ca^{2+}-sensitizing drugs which may bind to cTnC and increase cardiac output under conditions of cardiac failure. A variety of promising compounds have been identified including the diazinones pimobendan, MCI 154 and levosimendan. Design and screening of such drugs would be aided by an understanding of relationships between drug structure, drug binding sites on cTnC, and drug pharmacology. Toward this goal, we have assigned the Met methyl nuclei in [^{13}C-methyl]Met-labeled cTnC for use as structural markers for drug binding since they reside in hydrophobic regions on cTnC and may be sensitive to either direct interaction with the drugs or to shifts in the positions of neighboring Phe rings. HSMQC spectra show that bepridil and TFP cause very similar patterns of changes in the chemical shifts of N- and C- terminal Met resides, which is dominated by a striking broadening and shift for Met 45. In contrast, levosimendan, induces minimal broadening and much more modest changes in Met methyl chemical shifts, and it has no effect on Met 45. These data suggest that binding sites on cTnC for levosimendan are distinct from those of bepridil and TFP. Interpretation of the data relative to the solution structure of Ca^{2+}-bound cTnC suggest that bepridil and TFP bind to the limited N-terminal hydrophobic surface, which includes Met 45, in the N-terminus of cTnC.

Th-AM-A3

SLOW SKELETAL TROPONIN I GENE TRANSFER INTO ADULT CARDIAC MYOCYTES: THIN FILAMENT INCORPORATION AND ENHANCED CONTRACTILITY. ((M.V. **Westfall**, E.M. Rust, and J.M. Metzger)) Dept. of Physiology, University of Michigan, Ann Arbor, MI 48109

We used adenovirus-mediated gene transfer into highly differentiated adult rat cardiac myocytes to study the effect of slow skeletal troponin I (ssTnI) expression on myocyte structure and function. This approach resulted in rapid, uniform, and nearly complete replacement of the endogenous cardiac troponin I (cTnI) isoform with the ssTnI isoform within 7 days in primary culture. Importantly, there were no detected changes in the isoform composition or stoichiometry of other proteins in the contractile apparatus. Electron micrographs also indicated no change in sarcomeric ultrastructure compared to controls. In functional studies on permeabilized single cardiac myocytes, myofilament cooperativity (n_H) decreased and to a lesser extent, the Ca^{2+} sensitivity (pCa_{50}) of tension increased in ssTnI-expressing myocytes (n_H=1.6±0.2, pCa_{50}=5.97±0.06, n=14) relative to control values (n_H=3.0± 0.2, pCa_{50}=5.80±0.03, n=12). Thus, the threshold for Ca^{2+}-activated contraction was significantly lowered in adult cardiac myocytes expressing ssTnI. The tension-Ca^{2+} relationship was unchanged from controls in primary cultures of cardiac myocytes treated with adenovirus containing the adult cardiac troponin T cDNA. Thus, changes in Ca^{2+} sensitivity and cooperativity within ssTnI-expressing cardiac myocytes were isoform specific and not due to nonspecific functional changes resulting from overexpression of a myofilament protein. Further, Ca^{2+}-activated tension was enhanced in cardiac myocytes expressing ssTnI (pCa_{50}=5.28±0.07) compared to control values (pCa_{50}=4.49±0.02) under conditions mimicking the acidosis (pH=6.20) found during myocardial ischemia. These results demonstrate: 1) the feasibility of viral-based gene transfer for contractile protein structure/function studies in adult cardiac myocytes and; 2) enhanced contractile sensitivity to Ca^{2+} activation under physiological and acidic pH conditions in adult rat cardiac myocytes expressing ssTnI.

Th-AM-A4

PHOTOCROSSLINKING OF SINGLE CYSTEINE TROPONIN-I MUTANTS TO ACTIN IN RECONSTITUTED THIN FILAMENTS ((**Y. Luo**, Y. Qian, J.-L. Wu, J. Gergely and T. Tao)) Muscle Res. Group, Boston Biomed. Res. Inst.; Depts of BCMP and Neurology, Harvard Med. Sch.; and Neurology Service, Mass. Gen. Hosp., Boston, MA 02114.

We have shown previously that the Cys133 region of TnI undergoes reciprocal Ca^{2+}-dependent movement with respect to actin and troponin-C (TnC). Here we further mapped the actin contact sites in TnI using a set of single Cys TnI mutants: TnI6, TnI48, TnI89, TnI104, TnI133 and TnI179, where the numbers refer to the positions of the Cys's. Each mutant was labeled with the photocrosslinker benzophenone-4-iodoacetamide, then reconstituted with TnC, troponin-T (TnT), tropomyosin and fluorescently labeled actin. After photolysis the crosslinked products were identified as fluorescent bands on SDS gels. TnI-actin crosslinking was the highest for TnI133 and TnI104, while that for TnI89 and TnI179 were much less but still clearly detectable. All the yields were significantly reduced in the presence of Ca^{2+}. Crosslinking to actin of TnI6 was negligible and that of TnI48 was not detectable. We also found that TnI6 primarily crosslinked to TnC and TnI48 to TnT, both with and without Ca^{2+}. These results could be interpreted as follows: Residues 6 and 48 in TnI's N-terminal region interact strongly with the other Tn subunits, and do not interact with actin regardless of Ca^{2+}. Residue 89, closer to the so-called inhibitory region (residues 96-116), and residue 179 at the C-terminal tip of TnI make weak contact with actin in the absence of Ca^{2+}. Residues 104 and 133 in the inhibitory and C-terminal regions of TnI, respectively, make extensive contact with actin, more so in the absence than in the presence of Ca^{2+}. Our findings are compatible with the hypothesis that the N-terminal region of TnI is anchored onto TnC and TnT irrespective of Ca^{2+}, while the inhibitory region and portions of the C-terminal region undergo Ca^{2+}-dependent switching between TnC and actin in the course of thin filament regulation. (Supported by AR-21673 and HL-05949)

Th-AM-A5

EFFECTS OF RECONSTITUTION WITH WILD TYPE AND MUTANT CARDIAC TROPONIN-I IN SKINNED SOLEUS MUSCLE FIBERS. ((**H. Kögler***, C. Plathow*, E. Al-Hillawi#, I.P. Trayer#, J.C. Rüegg*)) *Physiology II, INF 326, 69120 Heidelberg, FRG; #School of Biochemistry, Birmingham B15 2TT, UK

Using a modification of the vanadate method for the reversible extraction of troponin I from skinned cardiac muscle (Strauss et al., FEBS Lett. 310: 229-234, 1992) we almost completely extracted the slow skeletal isoform of troponin-I (ssTnI) and also some troponin-C (TnC) from permeabilized rat and rabbit soleus fibers. Reconstitution with a complex of recombinant human cardiac TnI (cTnI) and TnC (cTnC) restored the ability of the fibers to relax in Ca^{2+}-free solution, which transiently had been lost in the TnI-depleted state. We subjected soleus fibers reconstituted with cTnI to catalytic subunit of protein kinase A (PKA) in the presence of [γ-^{32}P]ATP. This clearly demonstrated substantial phosphate incorporation into TnI which was totally absent in control experiments on native soleus fibers carrying only the non-phosphorylatable skeletal isoform. Surprisingly, however, no significant change in Ca^{2+} sensitivity resulted from this phosphorylation. These results are in contrast to findings in native or cTnI-reconstituted cardiac fibers where PKA-treatment induced a rightward shift of the pCa-tension relation by 0.2 and 0.3 pCa units, respectively. Consistently, the Ca^{2+} sensitivity of soleus fibers reconstituted with mutant cTnI in which both adjacent phosphorylatable serine residues Ser^{23} and Ser^{24} had been replaced by aspartate did not differ from that found in fibers reconstituted with wild type cTnI. In a previous study (Dohet et al., FEBS Lett. 377, 131-134, 1995) we had shown that reconstitution with this mutant effectively mimics the Ca^{2+}-desensitizing effect of PKA-dependent phosphorylation in cardiac skinned fibers. Obviously, PKA-dependent cTnI phosphorylation only exerts its effects on force development in an environment of cardiac-specific proteins, suggesting that the cardiac-specific N-terminal extension of TnI has a specific contact site elsewhere in the cardiac troponin complex.

Th-AM-A6

INTERACTION BETWEEN PHOSPHORYLATION AND Ca^{2+} BINDING TO MYOSIN REGULATORY LIGHT CHAIN FROM SMOOTH AND STRIATED MUSCLE. ((**G.M. Diffee**, J.R. Patel, F.C. Reinach, X.P. Huang, M. L. Greaser and R.L. Moss)) Dept. of Physiology, University of Wisconsin, Madison, WI 53706.

Previous studies have suggested a regulatory role for Ca^{2+} binding to myosin regulatory light chain (RLC) in skeletal muscle fibers. We examined the extent of Ca^{2+} binding to myosin RLC in skinned psoas fibers under physiological conditions by loading fibers with both the caged Ca^{2+} chelator NP-EGTA and the Ca^{2+}-fluorophore fluo-3. Using a UV-flash lamp we photolyzed the NP-EGTA to rapidly elevate the [Ca^{2+}] from low resting values (pCa 6.7) to as high as pCa 5.5. We monitored the initial rise in the fluo-3 signal and then the fall in fluo-3 fluorescence as an index of Ca^{2+} binding to intracellular sites. Experiments were done following complete extraction of TnC in order to remove it as a potential binding site for Ca^{2+}. We examined Ca^{2+} binding before and after phosphorylation of both endogenous skeletal muscle RLC (skRLC) as well as smooth muscle RLC (smRLC) that had been exchanged into the psoas fibers. We found that phosphorylation of skRLC had no significant effect on its ability to bind Ca^{2+} in the range of pCa's we tested, but that phosphorylation of smRLC resulted in a significant increase in Ca^{2+} binding to the light chain. Our evidence suggests that the increased binding is due to specific binding at the Ca^{2+}/Mg^{2+} site on RLC since there was no effect of phosphorylation of a mutant smRLC with an altered divalent cation binding site. These results suggest that enhanced binding of Ca^{2+} to the RLC may be a part of the mechanism of phosphorylation induced potentiation of force. We have found that phosphorylation of the mutant smRLC with reduced divalent cation binding does not potentiate force in skeletal muscle fibers.

Supported by NIH AR08226 and HL47053

Th-AM-A7

THE CALCIUM INDUCED STRUCTURAL CHANGE THAT TRIGGERS SKELETAL AND CARDIAC MUSCLE CONTRACTION.

((Stéphane M. Gagné[1], Monica X. Li[1], Ryan T. McKay[1], Samuel K. Sia[1], Leo Spyracopoulos[1], John A. Putkey[2], Murali Chandra[3], R. John Solaro[3], Lawrence B. Smillie[1] and Brian D. Sykes[1])) [1]Department of Biochemistry and MRC Group in Protein Structure and Function, University of Alberta, Edmonton, Alberta, Canada, T6G 2H7, [2]Department of Biochemistry and Molecular Biology, University of Texas at Houston, [3]Department of Physiology and Biophysics, University of Illinois at Chicago, Chicago, Illinois, 60612.

The binding of calcium to the muscle protein troponin-C (TnC) induces a conformational change which alters its interaction with the inhibitory protein troponin-I (TnI) and ultimately leads to muscle contraction. Comparison of the structures of the apo- and calcium-saturated regulatory domain of skeletal TnC (sNTnC) allows us to define the primary structural change and to propose a mechanism for the direct coupling of calcium binding to this conformational switch. The structure of intact TnC reveals flexibility between the structural and regulatory domains necessary for the interaction of the protein with target proteins. NMR studies of the interaction of sNTnC with TnI define the site of binding of TnI to the hydrophobic surface of the 'open' structure resulting from calcium binding. The structure of the calcium-saturated E41A mutant of sNTnC supports the mechanism, and allows us to visualize the step-wise binding of calcium to the protein and concommitant structural changes. The structures of apo- and calcium-saturated regulatory domain of cardiac TnC (cNTnC) reveal differences with the skeletal protein which result from changes in the residues in calcium site I. This result both supports our mechanism for calcium-conformational switch coupling and helps explain the functional differences between cardiac and skeletal muscle.

Th-AM-A8

SKELETAL TROPOMYOSIN HAS NO DISTINGUISHABLE EFFECT ON AVERAGE ISOMETRIC FORCE AND UNLOADED ACTIN FILAMENT VELOCITY *IN VITRO*.

((**P. VanBuren**#, J. Haeberle, H. Rarick*, J. Solaro*, N. Alpert, D. Warshaw)) Depts. of #Medicine and Molec. Physiol. & Biophys., Univ. of Vermont, Burlington, VT; *Dept of Physiol. & Biophys., Univ. of Illinois, Chicago, IL.

Solution biochemistry suggests that tropomyosin alters the kinetics of the myosin cross-bridge cycle. Lehrer & Morris (1982) demonstrated cooperative activation of myosin ATPase in the presence of tropomyosin. Using the *in vitro* motility assay to probe the mechanics of the skeletal muscle cross-bridge cycle, Fraser & Marston (1995) showed that actin filament sliding velocity is not altered by the presence of tropomyosin. Here, we have determined tropomyosin's effect on the generation of force utilizing *in vitro* techniques that measure the average force of as little as 50 myosin cross-bridges. In this assay, an actin filament is attached to an ultracompliant glass microneedle (50-200nm/pN). The free end of the actin filament is allowed to engage a skeletal muscle myosin coated surface. Under these experimental conditions (ionic strength, 40mM; pCa >9), preliminary data indicate that skeletal muscle actin/tropomyosin filaments generate similar average isometric force and unloaded actin filament velocity when compared to actin filaments without tropomyosin. (Support: Burroughs Wellcome Fund to P. VanBuren)

Th-AM-A9

CHARACTERIZATION OF THE FUNCTIONAL PROPERTIES OF DOMAIN 4A (HUMAN 622-708) OF SMOOTH MUSCLE CALDESMON

((**Mohammed EL-Mezgueldi**, O'neal Copeland, Iain Fraser, Steven B. Marston and Pia Huber))
Cardiac Medicine, Imperial College School of Medicine at the National Heart and Lung Institute, Dovehouse Street, London SW3 6LY, U. K.

It was proposed some time ago that there are two actin binding regions in the C-terminal 150 aminoacids, tentatively located within domain 4A and 4B. Recent work has suggested that the actin binding and inhibitory activity of caldesmon involves 3 regions in the C-terminus, two in domain 4B (C-terminal 80 amino-acids) and one in domain 4A (the N-terminal half of domain 4). In this study we have explored the inhibitory roles of sequences from domain 4A. We expressed two fragments of human caldesmon corresponding to differents parts of domain 4A. These fragments are H10 (human 622-708 (chicken 566-651)) and H13 (human 622-726 (chicken 566-665)). A third fragment containing domain 3 and domain 4A, H12 (human 506-708 (chicken 476-651)) was also studied. None of the fragments inhibited the acto-S-1 ATPase in the absence of tropomyosin. However the fragments inhibited the acto-S-1 ATPase in the presence of tropomyosin and this inhibition was reduced by an increase of the ionic strength. H13 is a more potent inhibitor of the actomyosin ATPase then H10. This is may be due to a higher affinity to actin as the sequence 708-726 (651-665 in chicken) has been shown to bind to actin. H12 is also a more potent inhibitor than H10 and this involves that the sequence 506-622 (476-566 in chicken) corresponding to domain 3 may contributes to the tropomyosin dependent inhibition of caldesmon. We conclude that domain 4A of caldesmon alone is able to inhibit the actomyosin ATPase activity but only in presence of tropomyosin. In addition domain 3 which is not an inhibitor in itself can confer more tropomyosin dependent ATPase inhibitory activity on domain 4A.

SARCOPLASMIC RETICULUM

Th-AM-B1

CRYO-ELECTRON MICROSCOPY AND IMAGE ANALYSIS OF THE CARDIAC RYANODINE RECEPTOR.

((**M.R. Sharma**, R. Grassucci, H.-B. Xin*, S. Fleischer* and T. Wagenknecht)) Wadsworth Center, New York State Dept. of Health, Albany, NY 12201 and *Department of Molecular Biology, Vanderbilt University, Nashville TN 37234 (Spons. by P.F. Flicker)

The 3D architecture of the skeletal muscle ryanodine receptor (RyR1) has been characterized previously by image analysis and cryo-EM applied to detergent-solubilized specimens. However, comparatively little structural data is available for the cardiac isoform of the receptor (RyR2). RyR2s appear poorly preserved when prepared for cryo-EM by the procedure used for RyR1, which involves removal of phospholipids in the final purification step. Phospholipids, at the levels normally present during purification, cause an unacceptable reduction of contrast in cryo-EM. Since it is known that removal of phospholipids from RyR2 cause loss of function (Inui and Fleischer, *Meth. Enzymol.* 157:491), we developed a simple protocol to reduce the lipid concentration on the EM grid within a few seconds of being frozen. Micrographs of RyR2 prepared by the modified method showed much improved structural preservation, and were suitable for image processing. Comparison of averaged images of RyR1 and RyR2, viewed in projection along their fourfold symmetry axes, indicate that the architecture of the two receptors is very similar, albeit there are small differences, the significance of which remains to be established. Progress is currently being made on determining a three-dimensional reconstruction of RyR2.

Supported by the NIH AR40615 (TW) and HL32711 (SF), and American Heart Assoc. fellowship 960124 (MS).

Th-AM-B2

SCANNING MUTAGENESIS REVEALS AN ASYMMETRIC DISTRIBUTION OF FUNCTION IN THE TRANSMEMBRANE DOMAIN OF PHOSPHOLAMBAN.

((**Y. Kimura** and D. H. MacLennan)) Banting and Best Department of Medical Research, University of Toronto, Toronto, Ontario, Canada M5G 1L6

Phospholamban (PLN), a 52 amino acid, transmembrane protein, inhibits the Ca^{2+}-ATPase of cardiac sarcoplasmic reticulum (SERCA2) by lowering its affinity for Ca^{2+}. In earlier studies, we and others characterized a regulatory cytoplasmic interaction site between the two proteins and, in more recent studies, we demonstrated that functional interaction occurs in transmembrane sequences of PLN and SERCA2. In this study, we have characterized the functional residues in PLN between Leu^{31} and Leu^{52} using alanine-scanning mutagenesis. PLN inhibitory function was lost by mutation to Ala of Leu^{31}, Asn^{34} or Phe^{35}. PLN inhibitory function was diminished by mutation to Ala of Ile^{35}, Leu^{42}, Ile^{48}, Val^{49} or Leu^{52}. Each of these mutants was pentameric in SDS-PAGE. PLN inhibitory function was enhanced (supershifted) by mutation to Ala of Phe^{32}, Ile^{33}, Leu^{37}, Ile^{40}, Leu^{43}, Leu^{44}, Ile^{47}, Met^{50} or Leu^{51}. Each of these supershift mutants was either completely monomeric in SDS-PAGE (Leu^{37}, Ile^{40}, Leu^{44}, Ile^{47}) or retained only a small amount of pentamer, indicating instability of the pentamer. The periodicity of the inactive and supershift PLN mutants suggests that: (1) one transmembrane helical face is involved in pentamer formation; (2) the other transmembrane helical face is involved in inhibitory SERCA2 interaction; (3) monomeric helices are much more inhibitory to SERCA2 than pentameric helices. We propose that PLN inhibition of SERCA2 involves, first, depolymerization of PLN and, second, inhibitory interaction between the transmembrane sequence of PLN and SERCA2. (Supported by the HSFO)

Th-AM-B3

EFFECT OF PHOSPHORYLATION ON THE STRUCTURE AND OLIGOMERIC STATE OF FLUORESCENT-LABELED PHOSPHOLAMBAN

(Ming Li, Roberta Bennett, Laxma Reddy, Norberto D. Silva Jr.[†], Larry R. Jones[*], David D. Thomas) Dept. of Biochemistry, University of Minnesota Medical School, Minneapolis, MN 55455; [†]Dept. of Pharmacology, Mayo Foundation, Rochester, MN 55905; [*]Krannert Institute of Cardiology, Indiana University, Indianapolis, IN 46202.

Time-resolved fluorescence energy transfer (FET) was used to measure the oligomeric state of phospholamban (PLB), a regulatory protein in cardiac sarcoplasmic reticulum. The theory of FET was extended to incorporate not only the distance between donor and acceptor, but also the donor-acceptor combinations within an oligomer. PLB subunits were specifically labeled at Lys 3 with either fluorescent donor or acceptor, and then mixed at defined ratios. The lifetimes and amplitudes of the fluorescence decays were measured to calculate both the distance between the adjacent subunits (R), and the total number of subunits within the oligomer (N). The results show that PLB exists primarily as an oligomer (N>=3) in detergent (SDS) solution and in a lipid (DOPC) bilayer. Phosphorylation changes the fluorescence amplitudes, not the lifetimes, indicating that the primary change is in the oligomeric state of PLB (N), not its internal conformation (R). The changes in the fluorescence amplitudes correspond to an increase in the fraction of molecules that are oligomeric. Since PLB inhibits the Ca-ATPase before, but not after, phosphorylation, this change in the oligomeric state of PLB may play an important role in Ca-ATPase regulation.

Th-AM-B4

MODULATION OF CARDIAC RYANODINE RECEPTORS BY SORCIN, A CALCIUM-BINDING PROTEIN OF MULTIDRUG RESISTANT CELLS.

((**Andrew J. Lokuta**[*], Marian B. Meyers[#], Glenn I. Fishman[#], Paul R. Sanders[*] and Hector H. Valdivia[*])). [*]Department of Physiology, University of Wisconsin-Madison and [#]Department of Medicine, Albert Einstein College of Medicine, Bronx, New York.

Sorcin is a calcium-binding protein, initially identified in multidrug-resistant cells, and more recently shown to be present in normal tissues such as cardiac muscle (Meyers et al, *J. Biol. Chem.* **270**:26411, 1995). Immunoelectron microscopy and immunoprecipitations suggested an association of sorcin to cardiac ryanodine receptors (RyR). We have investigated a possible functional interaction between sorcin and RyR using purified recombinant sorcin in [^{3}H]ryanodine binding experiments and single channel recordings of RyR. Recombinant sorcin completely *inhibited* [^{3}H]ryanodine binding with an $IC_{50} \approx 800$ nM. The open probability (P_o) of single RyR was also significantly *decreased* by addition of 600 nM to 1 μM sorcin to the cis (cytoplasmic) side. Sorcin-modulated RyR were still Ca^{2+}-dependent, but the degree of inhibition was constant over a wide range of [Ca^{2+}]. Furthermore, caffeine-activated RyR were also inhibited by sorcin when the [Ca^{2+}] was low (pCa 7). These results suggest that Ca^{2+} is not an obligatory factor for sorcin regulation of RyR. Rapamycin-treated RyR displayed higher [^{3}H]ryanodine binding than untreated RyR but no difference in their ability to interact with sorcin. Interestingly, prior phosphorylation of sorcin with the catalytic subunit of PKA abrogated sorcin's ability to inhibit RyR activity. Thus, sorcin is not only associated with cardiac RyR, but also has modulatory influences on channel activity. A potential role for sorcin in cardiac excitation-contraction coupling now warrants further investigation. Supported by NIH and the AHA.

Th-AM-B5

THE CARBOXYL-TERMINAL PORTION OF SKELETAL MUSCLE RYANODINE RECEPTOR FORMS A REGULATED CALCIUM RELEASE CHANNEL.

((**Manjunatha B. Bhat**, Jiying Zhao, Hiroshi Takeshima[*] & Jianjie Ma)), Dept. of Physiology & Biophysics, Case Western Reserve Univ., Cleveland OH, [*]Dept. of Pharmacology, Univ. of Tokyo, Japan.

The ryanodine receptor (RyR) is one of the key proteins involved in excitation-contraction coupling in skeletal muscle, where it functions as a Ca^{2+} release channel in the SR membrane. RyR consists of a single polypeptide of ~560 kDa normally arranged in a homotetrameric structure, which contains a carboxyl (C)-terminal transmembrane domain and an amino (N)-terminal cytoplasmic domain. To test whether the C- terminal portion of RyR is sufficient to form a Ca^{2+} release channel, we expressed the full length (RyR-wt) and C-terminal (RyR-C, ~130 kDa) RyR proteins in a chinese hamster ovary cell line, and measured their Ca^{2+} release channel functions in planar lipid bilayers. The single channel properties of RyR-wt and RyR-C are similar to those of RyR from skeletal muscle SR, including activation by micromolar Ca^{2+} and regulation by ryanodine. However, unlike RyR-wt which exhibits a linear current-voltage relationship and inactivates at millimolar Ca^{2+}, the channels formed by RyR-C display significant inward rectification and fail to close at high cytoplasmic Ca^{2+}. Our results show that the C-terminal portion of RyR contains structures sufficient to form a regulated Ca^{2+} release channel, but the N-terminal portion of RyR also affects the ion-conduction and Ca^{2+}- dependent regulation of the Ca^{2+} release channel. Supported by NIH, AHA, MDA, HHMI.

Th-AM-B6

LOCALIZATION OF CALMODULIN-BINDING DOMAINS IN THE SKELETAL MUSCLE SR CALCIUM CHANNEL PROTEIN.

((H.-C. Yang[1], Y.Wu[2], S.L. Hamilton[2], and **G.M. Strasburg**[1])) Michigan State University[1], East Lansing, MI 48824; and Baylor College of Medicine[2], Houston, TX 77030

Previous studies have shown that the skeletal muscle SR Ca^{2+}-channel protein binds 16 to 20 calmodulin (CaM) molecules per channel protein tetramer at [Ca^{2+}] corresponding to that of resting muscle [Yang et al., *Biochemistry* 33:518 (1994); Tripathy et al., *Biophys. J.* 69:106 (1995)]. This study was initiated to localize the CaM-binding domains in the primary structure of the native SR Ca^{2+}-channel protein. The channel protein in rabbit skeletal muscle SR vesicles was crosslinked (in the presence of 1 mM EGTA) with ^{125}I-labeled wheat germ CaM derivatized at Cys-27 with benzophenone-4-maleimide (^{125}I-Bz-CaM). The SR vesicles were briefly treated with calpain, and the proteolyzed channel protein crosslinked with ^{125}I-Bz-CaM was purified by sucrose gradient centrifugation. Autoradiography of SDS-PAGE gels coupled with western blots using site-specific antibodies were used to identify CaM binding domains. The M_r = 480,000 band, the largest fragment which bound ^{125}I-Bz-CaM, comprises amino acid residues ~1333-5037. The M_r = 173,000 fragment, which includes residues 1- ~1333 did not bind ^{125}I-Bz-CaM. Continued proteolysis of the 480,000 polypeptide resulted in a fragment of M_r = 365,000 comprising residues ~1333 - ~4400 which bound ^{125}I-Bz-CaM, plus a C-terminal fragment including residues ~4400-5037 which did not bind CaM. The M_r ≈ 365,000 fragment was sequentially cleaved to yield N-terminal fragments of first, 210,000 and then, 130,000; both fragments bound ^{125}I-Bz-CaM. Thus, the smallest CaM-binding fragment obtained by calpain digestion is localized to residues ~1333 to ~2600. These results further suggest that CaM-binding under these conditions is excluded from the N-terminal ~1300 residues and the C-terminal ~1000 residues.

Th-AM-B7

INTRACELLULAR CALCIUM HOMEOSTASIS IN HUMAN PRIMARY MUSCLE CELLS TRANSFECTED WITH THE WILD TYPE AND MUTATED RYR cDNA: EFFECTS OF HALOTHANE.

((**S. Treves**[1], K. Censier[2], A. Urwyler[2] and F. Zorzato[1])) [1]Institute of General Pathology, Univer. of Ferrara, Ferrara, Italy; [2]Department of Anaesthesiology, Kantonsspital/University of Basel, Basel, Switzerland.

Malignant hyperthermia is an inherited neuromuscular disease triggerred by volatile anaesthetics and myorelaxants. Eight point mutations in the skeletal muscle ryanodine receptor (RYR) gene have so far been identified and shown to correlate with malignant hyperthermia susceptibility (MHS). However, direct evidence linking abnormal $[Ca^{2+}]_i$ homeostasis to mutations in the RYR cDNA has been obtained for one such mutation (Arg615>Cys); in this case either COS-7 or C_2C_{12} cells were used to express the recombinant RYR. Experiments performed in our laboratories demonstrate that human skeletal muscle cells derived from MHS individuals present abnormal increases of $[Ca^{2+}]_i$ when challanged with halothane, compared to muscle cells from MHN individuals. The use of skeletal muscle-derived cultures for the expression of the RYR is much more appealing than that of other cell lines, especially in view of the fact that numerous muscle-specific proteins including FK506BP, triadin and the subunit of the DHPR have shown to interact with, stabilize and modify the function of the RYR Ca^{2+} channel. We present evidence which demonstrates that MHN and MHS-derived primary muscle cell cultures transfected with the wild type or mutated RYR cDNA express the recombinant RYR and. that the $[Ca^{2+}]_i$ response to halothane challenges differs in mock transfected MHS and MHN cells compared to cells transfected with the wild type or mutated RYR cDNA.

Th-AM-B8

INTERACTION OF NITRIC OXIDE WITH THE SKELETAL MUSCLE Ca^{2+} RELEASE CHANNEL.

((**Bahman Aghdasi**[#], Michael Reid[#,*] and Susan L. Hamilton[#])) [#]Department of Molecular Physiology and Biophysics, [*]Department of Medicine, Baylor College of Medicine, Houston Texas 77030.

N-Ethylmaleimide (NEM), a sulfhydryl alkylating agent, has three distinct functional effects on the Ca^{2+} release channel (CRC). NEM first inhibits both channel activity and [^{3}H]ryanodine binding (phase 1). With continued incubation it enhances both binding and channel activity (phase 2) and, finally, it again inhibits binding and channel activity (phase 3). Diamide, a sulfhydryl oxidizing agent, activates the channel, produces crosslinks between subunits within the tetramer of the CRC, and blocks phase 1 effects of NEM. Nitric oxide (NO) generating compounds prevent phase 1 effects of NEM and block intersubunit crosslinking. S-Nitroso-N-acetyl-D,L-penicillamine (SNAP) and PAPA NONOate (NOC-15) block intersubunit crosslinking at concentrations which have no detectable effects on the CRC activity. These reagents, however, do prevent the activation of the channel by diamide. The ability of NO donors to block intersubunit crosslinking within the tetrameric channel suggests that the sulfhydryls involved could be located at a subunit-subunit boundary. MAMA NONOate (NOC-9) and higher concentrations of NOC-15 activate the CRC. NO, therefore, appears to have more than one functional effect on CRC. In summary our data suggest that NO can react with phase 1 sulfhdryls at subunit-subunit contact domains to block the effect of oxidants. This reaction does not appear to alter channel activity. Higher concentrations of NO donors, however, activate the CRC.

[*]This work is supported by grants from the Muscular Dystrophy Association and the National Institutes of Health (AR41802) to SLH and the National Institutes of Health (HL45721) to MBR

Th-AM-B9

GENISTEIN INHIBITS SEROTONIN-ACTIVATED CALCIUM INFLUX THROUGH L-TYPE CALCIUM CHANNELS AND CALCIUM RELEASE FROM THE SARCOPLASMIC RETICULUM IN A10 VASCULAR SMOOTH MUSCLE CELLS. ((S. R. Nelson, T. Chien and **J. Di Salvo**)) Physiol., Univ. of Minnesota, Minneapolis, MN 55455.

Recent studies showed serotonin (S) induces protein tyr-phosphorylation in vascular smooth muscle cells. This suggested S-activated tyr-kinase activity may be coupled to influx of extracellular Ca^{2+} and release of intracellular Ca^{2+}. We sought to characterize the types of S-activated influx and release pathways blocked by genistein (G), an inhibitor of tyr-kinase activity, in rat aortic A10 cells loaded with fura-2. S evoked a large transient increase in $[Ca^{2+}]_i$, followed by a smaller sustained increase. Influx during the transient was inhibited by L-type Ca^{2+} channel antagonists (nicardipine, verapamil, and diltiazem), and essentially eliminated by G. In contrast, influx during the sustained response was unaffected by L-channel antagonists, and only slightly inhibited by G. In the absence of extracellular Ca^{2+}, the transient was inhibited by 50%, whereas the sustained component was virtually abolished. Thus, the transient involves influx and release, while the sustained response is due to influx only. Release was (a) blocked by G, (b) prevented by 2 μM thapsigargin, an inhibitor of Ca^{2+}-ATPases in the sarcoplasmic reticulum (SR), and (c) inhibited by 20 mM caffeine, a compound that activates ryanodine (R) receptors but inhibits inositol 1,4,5-triphosphate (IP_3) receptors. A10 cells expressed R and IP_3 receptors. In summary, different Ca^{2+} influx pathways are used during the transient and sustained components of the Ca^{2+}-response. Tyr-kinase activity probably participates in regulating (a) influx through both L-type Ca^{2+} channels and a non-L-type pathway, and (b) release of Ca^{2+} from caffeine-sensitive stores in the SR containing R and IP_3 receptors.

SYNAPTIC CHANNELS AND MEMBRANE RECEPTORS

Th-AM-C1

NON-REVERSIBLE NICOTINIC ACETYLCHOLINE RECEPTOR ACTIVATION

((**D. J. Maconochie** and J. H. Steinbach)) Cell Physiology and Pharmacology, Leicester University, LE1 9HN, UK and Anesthesiology, Washington University, St Louis MO 23110.

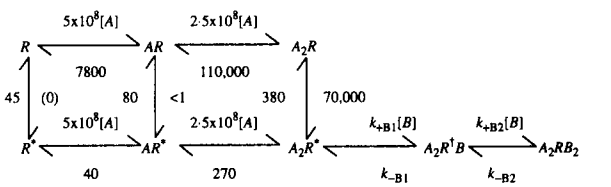

Figure 1. Units are $M^{-1}s^{-1}$ or s^{-1}. R^* is open channel, $R^\dagger$ and R are partially closed and closed channels respectively, A an activating ligand and B a blocking ligand.

We have examined the current recorded from outside-out patches isolated from cell lines expressing the adult (QA33) or fetal (QF18) complement of nicotinic receptor subunits. The averaged current immediately following either the application or the removal of ACh may be represented by sums of exponentials. We have charted the exponential rate constants and peak amplitudes as functions of ACh concentration. We find that a reversible Monod-Wyman-Changeux (MWC) model cannot predict the three exponential relaxations in the current on the removal of ACh, neither can a linear Castillo and Katz model or a two subunit Hodgkin-Huxley model. In contrast, the irreversible MWC model of figure 1. can predict almost every aspect of our data.

In this model, the doubly liganded opening rate is 70,000 s^{-1} for fetal and adult types, and mono and non-liganded opening rates are close to zero. We also find to our surprise that for low agonist concentrations ([ACh]<100 nM), the non-liganded open state is predicted to be long-lived, with a lifetime of 20 ms (Q_f,-60 mV). The lifetime of the mono-liganded open state is around 8 ms, and that of the di-liganded open state around 1.6 ms.

Th-AM-C2

INHIBITION OF THE NICOTINIC ACETYLCHOLINE RECEPTOR BY POLYAMINES: INVESTIGATED BY A LASER-PULSE PHOTOLYSIS TECHNIQUE. ((V. Jayaraman,[1] J. Ponasik,[2] B. Ganem,[2] P. N. R. Usherwood,[3] and G. P. Hess[1])) [1]Sect. of Biochemistry, Molecular and Cell Biology, Cornell University, Ithaca, NY. [2]Dept. of Chemistry, Cornell University, Ithaca, NY. [3]Dept. of Life Science, University of Nottingham, Nottingham, UK.

The mechanism of inhibition of a nicotinic acetylcholine receptor (nAChR) by polyamines containing aromatic moieties, such as philanthotoxin-343, kukoamine and some synthetic analogs, has been investigated using a laser-pulse photolysis technique, with a microsecond time resolution, in combination with a rapid cell-flow technique. The results indicate that in the presence of philanthotoxin-343 the nAChR channel-opening rate constant (k_{op}) decreases with increasing inhibitor concentration there is, however, no significant effect on the channel-closing rate constant (k_{cl}). In the presence of kukoamine both k_{op} and k_{cl} decrease with increasing inhibitor concentration. Determination of the dissociation constants for philanthotoxin-343 and kukoamine binding to the closed- and open-channel forms of the nAChR indicated that they had a six- and ten-fold higher affinity respectively for the closed-channel form than for the open-channel form. These results imply that the mechanism of inhibition by these polyamines is predominantly through inhibitor binding to the closed-channel forms of the nAChR. Studies with the synthetic analogs indicated that the secondary amines in the polyamine backbone were involved in the inhibition. Furthermore, these polyamines competed with cocaine, which is also an inhibitor of the nAChR.

We thank Dr. Kan Fang (from Prof. Nakanishi's laboratory, Dept. of Chemistry, Columbia University) for synthesizing philanthotoxin-343. This work was supported by a grant to G.P.H. from NIH (NS08527) and V.J. was supported by a Fellowship from the Cancer Research Fund of the Damon Runyon-Walter Winchell Foundation.

Th-AM-C3

DETERMINANTS OF AGONIST SELECTIVITY IN THE GAMMA AND DELTA SUBUNITS OF THE NICOTINIC ACETYLCHOLINE RECEPTOR (nAChR) AFFECT THE KINETICS OF ACTIVATION

((**R.J.Prince** and S.M.Sine)) Receptor Biology Laboratory, Mayo Foundation, Rochester, MN 55905

We recently identified four pairs of residues in the γ and δ subunits of the nAChR that confer selectivity of agonists for the two binding sites. Here we show that the two primary determinants of selectivity, γK34/δS36 and γF172/δI178, contribute to the kinetics of nAChR activation. We expressed either wild type or mutant AChR subunit cDNAs in 293 HEK cells and examined the single channel current kinetics using the patch clamp. Receptors containing γ(K34S + F172I) exhibited an EC_{50} for activation of less than 1 μM, compared to the wild type value of 10 μM. Conversely, receptors containing δ(S36K + I178F) exhibited an EC_{50} of greater than 100 μM (Figure). The results indicate that γK34/δS36 and γF172/δI178 contribute to the affinity of the activatable state of the AChR. Kinetic analysis currently in progress should allow identification of the step in the activation scheme affected by these determinants. Supported by NIH grant NS31744 to SMS and by the Myasthenia Gravis Foundation (RJP).

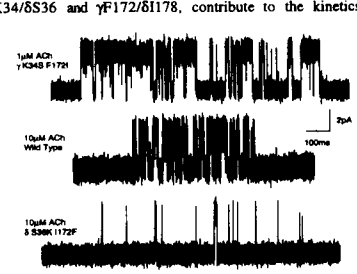

Th-AM-C4

NMDA RECEPTOR STOICHIOMETRY DETERMINED BY SUBCONDUCTANCE PATTERN ANALYSIS ((L. Premkumar, K. Erreger, and **A. Auerbach.**)) Department of Biophysical Sciences, SUNY at Buffalo, NY 14214.

The stoichiometry of NMDA receptor channels is not known with certainty. We have determined the subunit copy number for recombinant mouse NR1-NR2B receptors expressed in oocytes from the single-channel subconductance patterns (outside-out patches, -80 mV, 23 °C) arising from channels with wild type (N at the QRN site) and/or mutant (Q) subunits. First, all-N or all-Q subunit cRNAs were injected, resulting in the expression of four receptor classes (as NR1/NR2: N/N, N/Q, Q/Q, Q/N). All four types had a unique conductance signature, suggesting that the subunits assemble into a single order. Second, the NR1 subunit was all-Q, while the NR2 subunit was a 1:1 mixture of N and Q. Three types of conductance pattern were apparent. One was identical to the Q/Q pattern, and another was the same as the Q/N phenotype. We associate the novel conductance pattern (with 3 open channel conductances) with receptors having one Q and one N NR2 subunit (Q/(QN)), and conclude that there are two NR2 subunits per receptor. Third, the NR2 subunit was all-Q, while NR1 was a 1:1 mixture of N and Q. Four subconductance phenotypes were observed. One was identical to the Q/Q pattern, and one was the same as the N/Q phenotype. We associate the remaining two novel patterns with receptors having Q_2N and N_2Q stoichiometry for the NR1 subunits, and conclude that there are three NR1 subunits per receptor. We could identify each of these novel patterns with a particular subunit copy number by varying the injection ratio of N and Q NR1 subunits. By addition, we conclude that the NMDA receptor channel is a pentamer.

The amplitude and kinetic properties of each phenotype is under investigation. Models were selected after exhaustive likelihood comparisons of all possible connection schemes. Q/Q receptors have two open conductances (7.7 and 5.0 pA) that interconvert at ~300 s^{-1}. Q/(QN) channels have three open conductance levels (7.8, 6.9, and 3.2 pA), and have transition rate constants between states of increasing conductance of ~150 s^{-1}, and to lower conductance states of ~350 s^{-1}. We are trying to formulate physical models that account, in a simple way, for the kinetic information.

Th-AM-C5

RESIDUES IN M1 AND M2 ESSENTIAL FOR FUNCTION OF THE GABAA RECEPTOR

((**B.A. Cromer**, M.L. Tierney, S.M. Howitt, B. Birnir, P.W. Gage, and G.B. Cox)) JCSMR, ANU, Canberra, Australia. (Spon. by A. Dulhunty)

The γ-aminobutyric acid receptor, type A (GABAA Receptor) is a ligand-gated ion channel that, in response to binding of GABA, opens a chloride specific transmembrane channel within the receptor protein. It is the major channel protein involved in inhibitory synaptic transmission in the central nervous system. To determine the role of specific amino acid residues in ion conduction and channel gating, we have mutated selected residues in hydrophobic regions M1 and M2 of a model recombinant GABAA receptor. This model receptor is produced in Spodoptera frugiperda (Sf9) insect cells infected with a recombinant baculovirus that drives coexpression of the human α1 and β1 GABAA subunits. Mutation of the 10'T on the polar face of M2, α(T265A), β(T260A) increases the rate of desensitisation without affecting ion conduction. The mutations α(Q229L), β(Q224L) at the start of M1 and α(R274Q), β(R269Q) at 19' position of M2 abolish ion conduction in a subunit specific manner. We are able to show through immunofluorescence microscopy, flow cytometry and ligand binding assays that these mutant receptors are assembled and trafficked normally, indicating that these mutations directly affect receptor function. Mutation of the conserved proline in the M2-3 loop α(P278L), β(P273L) disrupts receptor maturation so that it no longer reaches the plasma membrane.

Th-AM-C6

ESTIMATING THE MICROSCOPIC BINDING RATE OF THE GABA$_A$ RECEPTOR.

((**Mathew V. Jones** and Gary L. Westbrook)) The Vollum Institute, Portland, OR 97201 (Spon. Gary L. Westbrook)

The microscopic binding and unbinding rates of the $GABA_A$ receptor are more relevant than the equilibrium affinity constant in determining the size and duration of inhibitory synaptic currents. We used fast ligand applications to voltage-clamped outside-out patches from cultured rat hippocampal neurons to measure the unbinding and binding rates of the competitive antagonist SR-95531 (SR)[1]. We then derived the binding rate of GABA from simultaneous applications of GABA and SR, in which the ligands "race" each other to their binding site.

Our methods were identical to those described previously[2]. SR unbinding was studied by preequilibrating a patch in saturating SR (10μM), then jumping out of SR and testing the fraction of unblocked receptors with saturating pulses of GABA (10mM, 20ms) after a variable interval. Peak GABA currents recovered exponentially with increasing SR unbinding intervals (Fig.1, τ_u=105±29ms (fit ± s.d. of fit), n=4). To study SR binding, a patch was exposed to 200nM SR for a variable interval, and then tested with GABA. Currents declined with increasing SR binding intervals (Fig.1, τ_b=43±27ms, n=7), to 51±3% at steady-state. Assuming a single antagonist binding site, SR has an unbinding rate (k_{off}) of $1/\tau_u$=9.5s^{-1} and a binding rate (k_{on}) of $(1/\tau_b - k_{off})/[SR]$=6.7x$10^7 M^{-1}s^{-1}$. The predicted equilibrium constant ($K_b=k_{off}/k_{on}$) is 142nM, consistent with published values[1] and with the steady-state block at 200nM, suggesting that the single-site model is a good first approximation. Simultaneous application of 1mM GABA and SR should therefore produce a current (I_{Race}) proportional to the ratio of their binding rates, such that $k_{on(GABA)}=k_{on(SR)}/((1/I_{Race})-1)$. I_{Race} was 8±2% (n=5) of the current for GABA alone (Fig. 2), giving a GABA binding rate of 5.8x$10^6 M^{-1}s^{-1}$. We predict that channels that unbind GABA after a single burst of openings[2] (~22ms) will have an apparent K_b of ~8μM, whereas those that unbind after a cluster of bursts[2] (~231ms) will appear to have a higher affinity, with a K_b of ~750nM. Refs: 1) Hamann et al. (1988) *Brain Res.* 442, 287-296. 2) Jones & Westbrook (1996) *Neuron* 15, 181-191. Supported by a Tartar Trust Fellowship (M.V.J.) and NS26494.

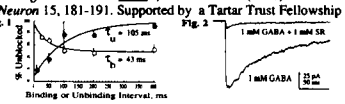

Th-AM-C7

THE ROLE OF CHARGED AMINO ACID RESIDUES IN PERMEATION AND BLOCK OF NEURONAL GLUTAMATE (AMPA/KA) RECEPTOR CHANNELS

((D. Gremmels, M. Hollmann# and B.U. Keller)) Zentrum Physiologie, Humboldtallee 23, University of Göttingen, #MPI for experimental Medicine, 37073 Göttingen, Germany.

The structure/function relationship of neuronal glutamate receptor channels was investigated by expressing wild type and mutant glutamate receptors GluR1 - GluR6 (GluR1 - GluR4 are alternatively noted as GluRA - GluRD) in *Xenopus* oocytes. Site - directed mutagenesis experiments were performed on charged amino acid residues between positions 540 - 594 (MII) that are commonly associated with the ion channel pore. If the basic functional properties of mutants were comparable to those of wildtype receptors, their response profile was analysed with respect to three functional properties: i) inward directed cation conductance ii) extracellular block by positively charged polyamine toxins and iii) outward directed cation conductance at positive membrane voltages. The results support a model of the glutamate receptor where the ion channel pore is formed by amino acid position 568-594 folding into the membrane from the cytoplasmic side.

Th-AM-C8

IN VITRO SELECTION OF PEPTIDE LIGANDS FOR PDZ DOMAINS.

((**Nicole Stricker**[1], Peter Schatz[2], Ron Raab[2], Karen Christopherson[3], David Bredt[3], Min Li[1]. [1]Departments of Physiology and Neuroscience, Johns Hopkins University School of Medicine, 725 N Wolfe Street, Baltimore, MD 21205; [2]Affymax Research Institute, Palo Alto, CA 94304; [3]Department of Physiology and Program of Biomedical Sciences, University of California, San Francisco, CA 94143))

Modular PDZ domains have been found in many proteins with diverse biological functions. Each of these protein modules consists of 90-100 amino acids and is thought to function by specific binding to a small carboxy-terminal peptide of target protein. To systematically determine the peptide binding specificity we have constructed random peptide libraries in which the random peptides were genetically fused to the C-terminus of the bacterial *lac* repressor. The DNA binding activity of the repressor protein physically links the peptides to the plasmid encoding them by binding to the *lac* operator sequence on the plasmid. This linkage allows efficient enrichment for specific peptide ligands in the random population by affinity purification of the peptide-repressor-plamid complexes with immoblized receptor. Using this approach, we have determined the optimal binding substrates of a PDZ domain present in neuronal nitric oxide synthase. Our data demonstrate that PDZ domains can be divided into different subclasses that possess different peptide-binding specificity.

REGULATION OF ION CHANNELS

Th-AM-D1

IDENTIFICATION OF DOMAINS THAT MEDIATE THE INHIBITION OF THE ROD CYCLIC NUCLEOTIDE-ACTIVATED CATION CHANNEL BY CALCIUM-CALMODULIN

((**M.E. Grunwald**, W.-P. Yu, J. Li, K.-W. Yau)) Howard Hughes Med. Inst. and Dept. of Neurosci., Johns Hopkins University School of Medicine, Baltimore, MD 21205.

The native rod cyclic nucleotide-activated channel is inhibited by Ca^{2+}-calmodulin (Ca^{2+}-CaM) (Hsu & Molday, *Nature* 361:76-79, 1993, Hsu & Molday, *J. Biol. Chem.* 269:29765-29770, 1994), apparently through subunit 2 (or β) of the channel (Chen *et al.*, *PNAS* 91:11757-11761, 1994; Körschen *et al.*, *Neuron* 15:627-636, 1995). We report here the identification of domains on subunit 2 that are involved in this inhibition. The cDNAs encoding the human rod channel subunit 1 (hRCNC1) and partial subunit 2 (hRCNC2b) were transfected into HEK 293 cells, and sensitivity of the heteromeric cGMP-activated channel to calmodulin was tested on excised inside-out patches in the presence of 50 μM Ca^{2+}. Half-maximal inhibition of the expressed channel occurred at 10 nM calmodulin or less. When hRCNC1 was co-expressed with hRCNC2b mutants lacking an N- and an C-terminal region, the inhibition by Ca^{2+}-CaM completely disappeared. Deleting the N-terminal region alone led to an almost complete loss of the calmodulin-mediated inhibition, whereas deletion of the C-terminal region had a small effect. Peptides derived from these regions were shown to bind dansyl-CaM in the presence of Ca^{2+}. Recently, we have also cloned the full-length (240 kDa) rod channel subunit 2 from human retina, and we are in the process of examining its sensitivity to Ca^{2+}-CaM.

Th-AM-D2

A MUTANT Na CHANNEL WITH ENHANCED PHOSPHORYLATION BY MYOTONIC DYSTROPHY KINASE.

((**J.R. Miller**, M.J. Kupke, G. Meixell, Xu P., J. Gilbert, A.D. Roses, M.B. Perryman, J.R. Moorman)) University of Colorado, Duke University, University of Virginia.

Co-expression of myotonic dystrophy kinase (DMK) decreases amplitude of muscle Na currents in RNA-injected *Xenopus* oocytes, an effect requiring the phosphorylation site KKLGSKKPQK in the inactivation gate. To investigate the role of the upstream positively charged lysine residues in DMK substrate specificity, we prepared a mutant synthetic peptide *NN*LGSKKPQK and the corresponding full-length Na channel cDNA. We measured rates of peptide phosphorylation of the wild type and mutant by purified DMK, and recorded whole cell and single channel Na currents in RNA-injected oocytes. We found (1) the mutant peptide was phosphorylated at a higher rate than the wild type; (2) co-expression of DMK reduced amplitude of mutant Na currents more than wild type ($p<0.02$, rank sum test); (3) at a test potential of -20 mV, the single channel mechanism of the DMK effect was an increase in the number of null traces and patches with no channel activity, and a decrease in the number of bursts and openings per trace ($p<0.05$ for each). These effects were more pronounced on the mutant channels, especially the decrease in the number of null traces and bursts. We conclude (1) DMK phosphorylates the Na channel inactivation gate and (2) demonstrates different substrate specificity than protein kinases A or C, which require upstream positively charged residues.

Th-AM-D3

EFFECTS OF HALOTHANE ON OOCYTE-EXPRESSED μ1 SKELETAL MUSCLE Na CHANNELS: IMPORTANCE OF PROTEIN KINASE C. ((**J.P. Mounsey**, M.K. Patel, J.E. John, J.R. Moorman)) University of Virginia.

Modulation of protein kinase C (PKC) may be a final common pathway of general anesthesia. Na channels, a potential target for general anesthetics, are substrates for PKC. The figure shows the effect of halothane on *Xenopus* oocyte-expressed muscle Na channels alone (*left*) and co-expressing a PKC α isozyme (*right*). Records (normalized for amplitude) show superimposed the control current at 0 mV (a), after 10 min halothane (5%) (b), and 10 min wash (c). Halothane enhanced current decay in the oocyte coexpressing PKC but had no effect on Na channels alone. In 22-32 oocytes (5 frogs) decay half-times were (m±SD, msec) 10.5±1.9 control, 10.6±1.8 halothane and 10.0±1.8 wash for oocytes expressing Na channels alone, and 10.3±1.9 control. 7.8±1.9 halothane and 8.8±2.3 wash in oocytes coexpressing PKC ($p<0.001$, control/halothane comparison in the presence of PKC, *t* test). Halothane had no effect on a Na channel mutant lacking a PKC phosphorylation site in the inactivation gate (S1321A). Halothane may enhance Na current decay by direct stimulation of PKC, or may interact preferentially with phosphorylated channels.

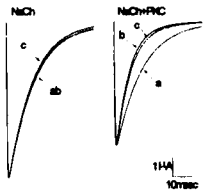

Th-AM-D4

THE EFFECT OF THYROID HORMONE ON THE TRANSIENT OUTWARD POTASSIUM CURRENT AND KV4.2 GENE EXPRESSION IN CULTURED NEONATAL RAT VENTRICULAR MYOCYTES.

((**A.D.Wickenden**, J.Tsoporis, T.G.Parker and P.H.Backx)) Centre for Cardiovascular Research, Division of Cardiology, The Toronto Hospital and Department of Medicine, University of Toronto, Toronto, CANADA. (Sponsored by B.Millman).

The transient outward potassium current (I_{to}) and its probable molecular correlate, Kv4.2, are strongly up-regulated with development in the rat heart. This is associated with accelerated repolarisation of the cardiac action potential. The factor(s) which mediate these developmental effects however, are not known. In the present study we investigated the effects of thyroid hormone on action potential characteristics, the biophysical properties of I_{to} and Kv4.2 gene expression in cultured ventricular myocytes from 1-2 day old rats. I_{to} density was 10.1 ± 1.6 pA/pF (n = 16) 24 h post-isolation and increased over 48-72h in culture under serum free conditions to 20.1 ± 3.0 pA/pF (n = 37). At all time-points following isolation, recovery from inactivation was biphasic with a prominent slow component. Following 48-72h under serum-free conditions τ_{fast} was 38ms (43%) and τ_{slow} was 7953 ms (51%; n = 6), the action potential was prolonged (APD_{90} = 168 ± 57 ms; n = 5) and showed pronounced rate dependent lengthening. Although I_{to} density (24.0 ± 2.9 pA/pF, n = 21) was unaffected, treatment with tri-iodothyronine (T3, 100nM) accelerated the rate of recovery from inactivation of I_{to} (τ_{fast} = 49.7 ms, 97% n = 9), reduced action potential duration (APD_{90} = 71 ± 14.6 ms; n = 4) and abolished rate dependence. I_{to} and action potential characteristics in T3 treated neonatal myocytes were very similar to those recorded from myocytes isolated from adult rat hearts. Quantitative RNase protection assays indicated that the effects of T3 were not associated with increased Kv4.2 transcript levels. In conclusion, T3 treatment mimics some of the electrophysiologic features of post-natal cardiac development.

Th-AM-D5

A-TYPE K⁺ CURRENT IN NEURONS CULTURED FROM NEONATAL RAT HYPOTHALAMUS AND BRAINSTEM: MODULATION BY ANGIOTENSIN II.

((Desuo Wang, Colin Sumners, Philip Posner, and **Craig H. Gelband**)) Department of Physiology, University of Florida College of Medicine, Gainesville, FL 32610.

The regulation of neuronal A-type K^+ current (I_A) and the single channel underlying I_A were studied using the patch clamp technique. When cells were held at -110 mV to relieve any voltage-dependent inactivation, I_A contributed approximately 30% to total outward current during voltage steps to membrane potentials greater than 0 mV (n = 5). I_A had a threshold of activation between -30 and -25 mV with a $V_{1/2}$ of +7.3 mV (n = 14). Steady-state inactivation of I_A occurred between -80 and -70 mV and had a $V_{1/2}$ of -52.2 mV (n = 14). Activation and inactivation time constants during a voltage step to +20 mV were 2.1±0.3 and 13.6±1.9 msec, respectively (n = 8). Single channel recordings revealed A-type K^+ channels with similar voltage-dependent activation and inactivation kinetics and 4-aminopyridine (4-AP) sensitivity to that of I_A. The single channel conductance obtained from cell-attached patches was 15.8±1.3 pS (n = 4) in a physiological K^+ gradient and was 41.2±3.7 pS (n = 5) in symmetrical 140 mM K^+. Pharmacologically, angiotensin II (Ang II, 100 nM) reduced peak I_A by approximately 20% (n = 8). Similarly, Ang II (100 nM) markedly reduced single A-type K^+ channel activity (n = 4). The actions of Ang II on I_A and single A-type K^+ channels were reversible either by addition of the selective AT_1 receptor antagonist, losartan (1 μM) or upon washout of the peptide. Thus, the activation of AT_1 receptors inhibits a TEA-resistant, 4-AP-sensitive I_A and single A-type K^+ channels and this may underlie some of the actions of Ang II on electrical activity of the brain. (Supported by NIH HL-49310, HL-52189 and an AHA Postdoctoral Fellowship, FL Affiliate)

Th-AM-D6

NOVEL STORE-OPERATED CATION CHANNELS MEDIATE AGONIST-INDUCED CALCIUM INFLUX AND CONTRACTION IN RABBIT AORTIC SMOOTH MUSCLE CELLS.

((**V.M.Bolotina**, R.M. Weisbrod, M.Gericke, P.Taylor, R.A. Cohen))
Vascular Biology Unit, Boston Medical Center, Boston, MA 02118, USA

Store-operated calcium influx is well described in non-excitable cells, but its nature and physiological significance in smooth muscle cells (SMC) is still unclear. Here we describe novel small (3 pS) non-selective cation channels (permeable to Ca^{2+}) which are regulated by the state of filling of IP_3-sensitive Ca^{2+} stores and mediate agonist -induced Ca^{2+} influx in rabbit aortic SMC. Using patch-clamp recording of single channels and whole-cell currents, and measurement of Ca^{2+} influx, intracellular Ca^{2+} concentration, and smooth muscle tension, we show that these channels, but not L-type Ca^{2+} channels, mediate agonist-induced inward current, calcium influx and contraction of rabbit aortic SMC. Single non-selective cation channels were activated in cell -attached patches following depletion of Ca^{2+} stores by either angiotensin II (AII) or thapsigargin (TG). AII and TG activated similar inward non-selective cation current and caused Ca^{2+} influx and Ca^{2+} rise which were inhibited by SKF 96365 and Ni^{2+}, but not by nifedipine. AII -induced Ca^{2+} influx was prevented by inhibition of IP_3-sensitive Ca^{2+} channels in intracellular stores with caffeine. Thus, agonist-induced Ca^{2+} influx and SMC contraction is mediated by small non-selective cation channels which are activated upon depletion of IP_3-sensitive Ca^{2+} stores, a process which can be promoted by TG or blocked by caffeine.

Th-AM-D7

DISTINCT AND SENSITIVE DETECTION OF HEAVY-METAL DIVALENT CATIONS USING A GENETICALLY ENGINEERED ION CHANNEL

((J.J. Kasianowicz[†] D.L. Burden[#], L.C. Han[†], S. Cheley[‡] and H. Bayley[‡]))
[†] NIST, [#] Indiana University and [‡] Worcester Foundation for Biomedical Research

The mean single channel current and current fluctuations of *Staphylococcus aureus* α-hemolysin (αHL) vary predictably with pH[1]. We're determining the ability of genetically engineered mutants of αHL to serve as rationally designed sensors for other cations (e.g. transition metal divalent cations)[2]. We show that [Zn] ≤ 1 mM had no effect on wild type-αHL's hemolytic activity or its single channel current and that metal ion binding sites were created by genetically engineering ionizable side chains into the protein. Metal-sensitive αHLs were screened by zinc's ability to inhibit their hemolytic activity and studied with single channel recording techniques. The point mutation G130H caused current fluctuations that varied with the concentration and type of divalent cation. Replacement of all the ionizable side chains near position 130 with non-ionizable counterparts (D127N, D128N, K131Q & H144N) abolished the channel's sensitivity to Zn. Subsequent placement of a single aspartic acid into the latter construct helped identify the minimum metal ion binding site. Specifically, introduction of D128 or G126D (but not D127) regained Zn sensitivity better than 1 μM. The latter results verify that the pore is lined by β-sheets[3] and that these sites span a reverse turn[3]. **References:** 1) Bezrukov, S.M. & J.J. Kasianowicz. 1993. *Phys. Rev. Lett.* **70**: 2352; 2) Walker, B., et al. 1994. *Protein Eng.* **7**: 655; 3) Song, L., et al. *submitted.* **Supported by** the NRC (JK), NSF (DB), DOE & ONR (HB).

Th-AM-D8

EFFECTS OF ABA ON INWARD RECTIFYING POTASSIUM CONDUCTANCE IN ALEURONE PROTOPLASTS FROM DORMANT AND NON-DORMANT BARLEY GRAINS.

((**Bert Van Duijn**, Marcel T. Flikweert and Mei Wang)) Center for Phytotechnology RUL/TNO, Waasenaarseweg 64, 2333 AL Leiden, The Netherlands.

To study the involvement of ion channels in the ABA-induced ion- concentration and -flux changes we applied the patch-clamp technique to barley aleurone protoplasts. Protoplasts obtained from aleurone of both dormant and nondormant grains (*Hordeum distichem* L. cv Triumph) were used to investigate whether ABA responsiveness differences, like exist for Rab gene expression, are also present for modulation of ion channels. In all types of protoplasts a time and voltage dependent inward directed current ($I_{K,in}$) through the plasma membrane could be measured. This current was hyperpolarization activated and showed a reversal potential that shifted with the potassium equilibrium potential.We compared the $I_{K,in}$ in the different types of protoplasts. From this we conclude that, taking the size of the protoplasts into account, the $I_{K,in}$ in protoplasts from dormant Triumph grains showed a much smaller $I_{K,in}$ than in protoplasts from non-dormant grains (Plant Growth Regul. 18:107-113, 1996). Addition of 5μM ABA resulted, in all types of protoplasts used, in a doubling of the maximal conductance of the $I_{K,in}$. The ABA responsiveness difference between aleurone protoplasts from dormant and nondormant grains could also be found in the ABA-induced increase in the $I_{K,in}$.

Th-AM-D9

AMMONIUM CHLORIDE DECREASES A VOLTAGE-SENSITIVE POTASSIUM CURRENT IN ISOLATED CORONARY SMOOTH MUSCLE MYOCYTES
((R.G. WEBSTER W.A. COETZEE* L.H.CLAPP)) Cardiovascular Research, Rayne Institute, St. Thomas' Hospital, London, SE1 7EH, UK, and *Pediatric Cardiology, NYU Medical Centre, NY, NY 10016, USA.

Ammonium chloride (NH_4Cl) causes intracellular alkalinization and vascular smooth muscle contraction, although the mechanism has not been fully elucidated. We investigated the effects of NH_4Cl (20 mM) on whole-cell current in isolated rabbit coronary myocytes using the patch clamp technique. Cells were voltage clamped at -50 mV (at 22°C) and ramped over a range of potentials from -120 to 60 mV (0.32 mV/msec). The intracellular pipette solution contained (in mM): KCl 140, Na-GTP 0.5, Mg ATP 3, EGTA 0.5, $MgCl_2$ 1, HEPES 20. In a physiological K^+ gradient NH_4Cl decreased current at all potentials above -60 mV, with greatest percentage decrease around the resting potential; at -40 mV outward current decreased by 45 ± 7 % (n=11, ± sem). Similar responses were obtained in the presence of nifedipine (5μM) (n=6). In 60 and 120 mM $[K^+]_o$ NH_4Cl-sensitive current reversed at -23 mV (E_K -21 mV), and -6 mV (E_K -4 mV), respectively. In 120 mM $[K^+]_o$ NH_4Cl affected a steeply voltage-gated K^+ current that activated above -85 mV and showed little inactivation over 1sec. The magnitude of the NH_4Cl-sensitive current at -75, -50, and -20 mV was -3.29±1.23, -15.84±2.55, and -6.94±1.58 pA/pF, respectively (n=4, ± sem). In conclusion, NH_4Cl decreases a voltage-sensitive potassium current which might be responsible for NH_4Cl-induced contraction in coronary vascular smooth muscle.

Supported by British Heart Foundation

MEMBRANE STRUCTURES

Th-AM-E1

THREE-DIMENSIONAL STRUCTURE OF A WATER CHANNEL, AQUAPORIN-1, AT 6.5Å RESOLUTION AS OBTAINED BY ELECTRON CRYSTALLOGRAPHY
((H.L. Li, S. Lee and B.K. Jap)) Life Sciences Division, Lawrence Berkeley National Laboratory, University of California, Berkeley, CA 94720

Aquaporin-1 is a class of water channels within the aquaporin superfamily that can be found, for example, in the cell membranes of many mammalian tissues and in the vacuolar membrane of plants. The function of these channel proteins is to facilitate the transport of water into and out of cells. We have purified aquaporin-1 from bovine red blood cell membranes and reconstituted the purified protein with lipid to form two-dimensional crystalline patches that diffract to a resolution of about 3Å. Using high resolution electron microscopy techniques, we have collected images of aquaporin-1 embedded in trehalose at various tilt angles to about 45 degrees. Images were processed to a resolution of about 6.5Å and were merged to obtain a three-dimensional (3-D) density map. The map shows that aquaporin-1 is a tetramer of cylinders, of which each monomeric cylinder has a trapezoid-like cross section. The wall of each cylinder is made up of six rod-like structures that can be interpreted as α-helices which traverse the membrane. Within each monomer there is an additional rod-like density, somewhat different in appearance from the six outer rods, that can also be interpreted in part as containing a transmembrane α-helix which appears to form a part of the channel itself. This 3-D map is consistent with our earlier report on the projection map of aquaporin-1, indicating that each monomeric protein contains more than six transmembrane α-helices.

Th-AM-E2

CRYSTAL STRUCTURE OF *USTILAGO MAYDIS* KP6 KILLER TOXIN ALPHA-SUBUNIT
((Naiyin Li[1], Chung-Mo Park[2], Mary Erman[1], Walter Pangborn[1], Jeremy A. Bruenn[3], William L. Duax[1] and **Debashis Ghosh**[1,3]))
[1]Hauptman-Woodward Medical Research Institute, Inc., 73 High Street, Buffalo, NY 14203; [2]Biological Sciences, State University of New York at Buffalo, Buffalo, NY 14226; [3]Roswell Park Cancer Institute, Buffalo, NY 14263.

The *Ustilago maydis* KP6 killer toxin is a virally encoded secreted protein that kills sensitive *Ustilago* cells. The toxin is unique in that a KP6 oligomer containing α- and β-subunits interacts with the cell membrane, apparently resulting in an efflux of potassium and death of the target cells. The X-ray crystallographic determination of the structure of the toxin has been undertaken in order to investigate the structure-function relationship of the toxin. The α-subunit, a 78 amino acid long polypeptide, has been crystallized in the hexagonal space group $P6_322$ with unit cell dimensions a=b=48.3Å and c=124.2Å, and one subunit in the asymmetric unit of the crystal. The structure has been determined from an electron-density map prepared by the multiple isomorphous replacement method using a platinum heavy-atom derivative and a seleno-methionine substituted toxin, follwed by solvent-flattening. The tertiary structure is comprised of a two-turn α-helix and a three-stranded β-sheet. The packing of the molecules in the crystal is such that six helices aggregate through the crystallographic symmetries. The model will be refined at 1.8Å resolution and details will be presented.

Th-AM-E3

CRYSTALLIZATION AND PRELIMINARY X-RAY CRYSTALLOGRAPHY OF A LOW DENSITY LIPOPROTEIN FROM HUMAN PLASMA.
((**Peter Laggner**,‡ Ruth Prassl,‡ Ajay Saxena,‡ Fabienne Nigon,† Margit Sara,# Susanne Eschenburg,§ Christian Betzel,§ and John M. Chapman†))
‡Institute of Biophysics and X-ray Structure Research, Austrian Academy of Sciences, Graz, Austria, †INSERM Unite 321, Paris, France, #Centre for Ultrastructure Research, Agricultural University, Vienna, Austria and § EMBL-Outstation, Hamburg, BRD

Single crystals of human plasma low density lipoprotein (LDL), the major transport vehicle for cholesterol in blood, have been produced with a view to analysis of the three-dimensional structure by X-ray crystallography. Crystals with dimensions of approximately 200x100x50 μm have been reproducibly obtained from highly homogeneous LDL particle subspecies, isolated in the density ranges d=1.0271-1.0297 g/mL and d= 1.0297-1.0327 g/mL. Electron microscopic imaging of ultrathin-sectioned preparations of the crystals confirmed the existence of a regular, quasihexagonal arrangement of spherical particles of approximately 18 nm in diameter, thereby resembling the dimensions characteristic of LDL after dehydration and fixation. X-ray diffraction with synchrotron radiation under cryogenic conditions revealed the presence of well resolved diffraction spots, to a resolution of about 29 Å. The diffraction patterns are indexed in terms of a triclinic lattice with unit cell dimensions of a=16.1 nm, b=39.0 nm, c=43.9 nm; α= 96.2°, β=92.1°, γ=102°, and with space group P1.

Th-AM-E4

CHARACTERIZATION OF NATIVE AND RECOMBINANT FORMS OF POR A AND POR B GENE PRODUCTS FROM *NEISSERIA MENINGITIDIS*.
((C.A.S.A. Minetti[1], M.S. Blake[1], J.Y. Tai[1] and D.P. Remeta[2])) [1]North American Vaccine Inc., Beltsville, MD 20705, and [2]NHLBI, National Institutes of Health, Bethesda, MD 20892

Previous studies from our laboratories have focused attention on the functional activity and conformational stability of Por B class 2 and class 3 proteins which are mutually exclusive integral outer membrane proteins from *Neisseria meningitidis*. Por A class 1 protein is an abundant outer membrane antigen within meningococcal strains that is not essential for bacterial survival. Several wild type and mutant strains lacking this protein appear to present all the basic porin mediated functions, including exchange of nutrients/waste products and sensitivity to hydrophilic antibiotics. Por A class 1 has been purified to homogeneity from a meningococcal mutant strain devoid of class 3 and class 4 proteins (i.e., 44/76 Δ3/Δ4). The recombinant counterpart has been overexpressed in *E. coli* as inclusion bodies and refolded by a detergent-assisted procedure developed for Por B rclass 2 and rclass 3 proteins [Qi et al., (1994) *Infec. Immun.* 62, 2432-2439]. Both the native and recombinant forms of Por A class 1 protein exhibit characteristic porin-like function (as measured by the liposome swelling assay) and structure (as monitored by circular dichroism, UV, and fluorescence spectroscopy). Comparison of thermal and guanidine-induced unfolding pathways suggests that Por A class 1 resembles Por B class 2 with respect to overall conformational stability [Minetti et al., (1996) *J. Biol. Chem.*, In press]. The results of our comparative studies are discussed in terms of available topology models for the Por A and Por B proteins which may facilitate elucidation of structure-stability relationships among neisserial proteins within the porin superfamily.

Th-AM-E5

MACROMOLECULAR ASSEMBLY OF LIPOPOLYSACCHARIDES

((**C. A. Aurell** and A. O. Wistrom)) College of Engineering, University of California, Riverside, CA 92521.

We have studied the macromolecular assembly of hydrated bacterial endotoxins or lipopolysaccharides (LPS), cell wall components of gram negative bacteria using autocorrelation and fluorescence spectroscopy. The purpose is to understand the fundamental mechanisms how LPS monomers assembly into intermediate macromolecular structures, the formation of LPS supramolecular assemblies and how of these physical changes of bacterial LPS conformation affect ligand-receptor interactions in the mammalian septic shock pathway. Earlier studies of the hydrated geometry of different LPS *(Aurell et al., Biophys.J. 70, 988-997,1996)* located fluorescent donor labels, fluorescein isothiocyanate (FITC) on LPS inserted in a detergent micelle (sulfobetaine palmitate) by steady-state fluorescence resonance and time-resolved fluorescence resonance energy transfer. Calculations of the geometry for LPS with long O-antigens suggested that the polysaccharide chains extended more than ~100 Å. In this study we determined the critical micelle concentration, CMC of hydrated LPS (*S.minnesota* Re 595) and its precursor Lipid A (*S.minnesota* Re 595) by N-P-N fluorescence and static light scatter measurements. The CMC's appears to be in the lower μM range, about 2 and 8 μM respectively. Autocorrelation spectroscopy was used to measure the particle size distribution and the mean hydrodynamic diameter of LPS fragments. The mean diameter for wild type LPS (*S.minnesota)* was about 76 nm compared to about 55 nm for the short polysaccharide chain LPS mutant strain (*S.minnesota* Re 595). The particle size distribution for Lipid A ranged from 500 nm to 10 μm, mean at about 8 μm. Results suggest that LPS fragment size and geometry depends on the LPS polysaccharide chain length and solubility.

Th-AM-E6

ANALYSIS OF FIBROBLAST PLASMA MEMBRANE STEROL-RICH DOMAINS USING SMALL ANGLE X-RAY SCATTERING APPROACHES

((A.T. Remaley*, P.E. Mason, C.M. DeRosia and **R.P. Mason**)) Neurosciences Research Center, Allegheny University of the Health Sciences, Allegheny Campus, Pittsburgh, PA and *NHLBI, NIH, Bethesda, MD.

It has been proposed that cellular efflux of unesterified (free) cholesterol to acceptor particles is influenced by its distribution in the plasma membrane. In this study, the structure of sterol-rich domains in human fibroblast cell plasma membranes was examined using small angle x-ray scattering (SAXS) techniques under physiological-like conditions. The plasma membranes were oriented by centrifugation and placed on a curved glass mount so that the plane of the membranes was oriented around an axis perpendicular to the incoming focused x-ray beam at discrete angles. At 20°C, plasma membranes isolated from cholesterol-loaded fibroblasts produced strong and reproducible reflections along the meridional axis, 1/34 and 1/17 $Å^{-1}$. A high angle reflection was also observed (1/5.7 $Å^{-1}$). These reflections indicate a sterol-rich domain consisting of a cholesterol "bilayer" in the plane of the membrane. The surrounding sterol-poor domain had a *d*-space of 55 Å. Plasma membrane structure was also examined following cellular cholesterol efflux (20 hr) to free apolipoprotein apoA-I. Following cholesterol efflux, the ratio of the diffraction intensities corresponding to the sterol-rich domain: sterol-poor domain decreased 70-fold and the *d*-space of the sterol-poor width increased to 60 Å. These findings were reproduced with model lecithin bilayers of various cholesterol content and provide direct evidence for sterol-rich domains in human fibroblast plasma membranes that are modulated by cholesterol efflux to lipid acceptor particles.

Th-AM-E7

CHOLESTEROL SULFATE HAS TWO LOCATIONS IN DMPC MEMBRANES. A STUDY BY NEUTRON DIFFRACTION AND MOLECULAR MECHANICS SIMULATION

((C. Faure, M. Laguerre, W. Néri, **E.J. Dufourc**)), CRPP-CNRS, Av. A. Schweitzer, 33600 Pessac, France.

A variance in the delicate balance of cholesterol (CH) versus cholesterol sulfate (CS) in spermatozoid membranes or in the stratum corneum may alter fusion of the former or trigger a disease of the latter otherwise known as ichtyosis[1-2]. It has recently been proposed that the very high hydration and swelling properties of CS in phospholipid membranes could condition such effects [3] and would result in a different vertical location of the steroid in the bilayer. Such an hypothesis was investigated by neutron diffraction using ring-deuterated and unlabelled CS embedded in macroscopically oriented membrane samples. Proton-deuterium contrast methods afforded the location of the labels and showed that about half of the CS is embedded as CH, that is with the polar moiety at the level of the fatty acyl carbonyl groups of DMPC, whereas the other half was 6 Å upper in the bilayer, i.e. in the aqueous compartment such that the sulfate group is in favorable interaction with the quaternary ammonium of the choline lipid head group. On the other hand, an energetic minimization was realized on fully hydrated DMPC lamellae containing the same CS content as for neutron experiments (33 mole %). The steroid was initially positioned as cholesterol, i.e., fully embedded in the bilayer. Once the optimal energetic situation is reached, CS molecules are found to be evenly distributed between the two locations as reported by neutron diffraction.

[1] Fayrer-Hosken, R.A., B.G. Brackett & J. Brown. 1987.*Biol. Reprod.* 36:878-883. [2] Rehfeld, S.J., M.L. Williams & P.M. Elias. 1986. *Arch. Derm. Res.* 278:259-263. [3] Faure, C., J.F. Tranchant & E.J. Dufourc, 1996, *Biophys. J.* 70:1380-1390.

THE MULTIDRUG RESISTANCE PROTEIN: PUMP OR PARADOX?

Th-AM-SymII-1 S. Ruetz, Ciba Geigy, Switzerland
Membrane Transport Catalyzed by P-glycoprotein

Th-AM-SymII-2 S. Simon, Rockefeller University
The Secretory Pathway in Chemotherapy and Drug Resistance

Th-AM-SymII-3 A. E. Senior, University of Rochester Medical Center
The Catalytic Cycle of P-glycoprotein

Th-AM-SymII-4 P. Roepe, Memorial Sloan-Kettering Cancer Center
The Altered Partitioning Model for MDR Protein

Th-AM-F1

HETEROLOGOUS EXPRESSION OF HUMAN β-CARDIAC MYOSIN IN MOUSE MYOBLASTS IN CULTURE; EFFECTS ON MYOBLAST MOTILITY AND DIFFERENTIATION. ((P. Taylor-Harris, C. Wells, D. Coles, P. Fraylich, D. Zicha, G. Dunn & **M. Peckham**)) The Randall Institute, King's College London, 26-29 Drury Lane, London, WC2B 5RL. UK.

We have constitutively expressed full length human β-cardiac myosin heavy chain (β-MHC) and truncated (β-HMM) in mouse myoblasts (*H2k*^{b}-tsA58; Morgan et al., (1994) Dev. Biol. **162**, 486-498) in culture. The β-MHC and β-HMM expressing myoblasts differentiate into myotubes with a normal striated appearance. The full length β-MHC integrates into the muscle sarcomere, whilst the truncated β-HMM does not, as expected. However, the rate of sarcomere development in these myotubes may be slower compared to wild type or sham transfected cells. Despite using a strong constitutive promoter, the levels of expression in permanently transfected clones were low. Time-lapse interference microscopy (Dunn & Zicha, (1995) J. Cell. Sci. **108**, 1239) of myoblasts showed that both the speed and the spread area to mass ratio of β-MHC and β-HMM expressing myoblasts was reduced to about 80% of that measured for wild type or sham transfected myoblasts. Immunofluorescence showed that β-MHC and β-HMM expressing myoblasts had reduced focal adhesions and actin stress fibres. These results suggest that the expressed β-MHC or β-HMM affects myoblast motility, spreading and possibly adhesion. Either the expressed myosin depletes light chains from the endogenous non-muscle myosin interfering indirectly with its interaction with actin, or it can affect the interaction of actin and non-muscle myosin directly. This dominant negative effect of expressed β-MHC and β-HMM could explain their low levels of expression; we may not be able to recover more highly expressing clones, because the high levels of expressed β-MHC or β-HMM prevent them from adhering to the surface.

Th-AM-F2

FUNCTIONAL CONSEQUENCES OF MYOSIN HEAVY CHAIN MUTATIONS IMPLICATED IN FAMILIAL HYPERTROPHIC CARDIOMYOPATHY
((H. Yamashita, S. Lowey, and K.M. Trybus)) Rosenstiel Research Center, Brandeis Univ., Waltham, MA 02254.

Various missense mutations in β-cardiac myosin heavy chain are associated with familial hypertrophic cardiomyopathy (FHC). To study the functional consequences of these mutations, we expressed gizzard smooth muscle heavy meromyosin in the baculovirus / insect cell system with Arg-406 mutated to Gln (equivalent to cardiac R403Q in FHC), Arg-731 to Gln (R719Q) or Trp (R719W), and Asp-789 to Gly (D778G). Unexpectedly, the R403Q mutant supported actin filament movement to a similar or slightly higher extent than wild-type (WT), despite its severe disease phenotype. Both R719Q and R719W exhibited a similar filament velocity to WT, whereas D778G showed a significantly higher value in the *in vitro* motility assay. Those mutations that resulted in higher velocities had correspondingly higher actin-activated ATPases. The higher velocity of the D778G mutant is of particular interest, since the mutation is at the top of the α-helix that binds the ELC and abuts the motor domain, a location that may be important for the rotation of the light chain binding domain or lever arm. These results may provide insights into which sequences of myosin are involved in energy transduction, and how mutations in these regions impact on normal muscle function.

Th-AM-F3

FAMILIAL HYPERTROPHIC CARDIOMYOPATHY (FHC) MYOSIN HEAVY CHAIN MUTATION D778G ALTERS UNITARY EVENT DURATIONS MEASURED IN THE LASER TRAP
((Matthew J. Tyska, Hiroshi Yamashita*, David M. Warshaw, and Kathy M. Trybus*)) Dept. Mol. Physiol. & Biophys., U. of Vermont, Burlington, VT 05405 and *Rosenstiel Res. Ctr., Brandeis Univ., Waltham, MA 02254.

FHC is an inherited cardiac disease that can arise from various missense mutations in the β-myosin heavy chain gene. To understand how these single point mutations affect the function of myosin at the molecular level, we used a laser trap to characterize the molecular mechanics of a D778G mutation (smooth D789G) in smooth muscle heavy meromyosin (HMM) expressed in an insect cell system. This mutation is located in the putative "fulcrum" that potentially transmits conformational changes within the catalytic domain to the neck (Rayment et al., 1993). Data from the D778G mutant suggest that while unitary forces (F_{ens}≈3.5 pN) and displacements (d_{ens}≈10 nm) appear to be unchanged, the average unloaded displacement event duration (t_{on}) is significantly shorter than that found for wild-type HMM (40-90ms vs. 160-200ms). This finding can explain the enhanced unloaded actin filament velocity (V_{actin}) for this mutant (Yamashita et al., see previous abstract) since $V_{actin}=d_{ens}/t_{on}$. These D778G data suggest that mutations in this region of myosin impact upon the kinetics of the crossbridge rather than its inherent force and motion generating capacity. Further characterization of D778G will enable us to better understand how this region is involved in chemo-mechanical transduction.

Th-AM-F4

DETECTION OF THE 606 VAL→MET MUTATION IN HUMAN β-MYOSIN HEAVY CHAIN AT THE PROTEIN LEVEL BY MASS-SPECTROMETRY (V. Nier*, M. Raida*, T. Kraft*, E. Thedinga*, W.G. Forssmann*, W.J. McKenna[§], B. Brenner*) *Dept. Clin. Physiol., MHH, 30623 Hannover, *Lower Saxony Institute for Peptide Research, 30625 Hannover (Germany), [§]Department of Cardiological Sciences, St. George's Hospital Medical School, London

Missense mutations in the β-myosin heavy chain are observed in familial hypertrophic cardiomyopathy (FHC). Surprisingly members of different families with the same mutation, and even members of the same family exhibit a great variation in symptoms. Cuda et al. (JMRCM 15: 1994) reported a reduced *in vitro* sliding velocity with myosin from patients with the 606 Val→Met mutation in the β-myosin heavy chain. In contrast myosin with the same mutation but from an asymptomatic patient from another family showed no difference in *in vitro* sliding velocity to control myosin, and no differences in isometric force, unloaded shortening velocity and the rate constant of force redevelopment were found (Kraft et al., Biophys. J. 70: A41, 1996). Similar to the discrepancy with Cuda's results the clinical symptoms are different between the two families. These differences may be due to variation in expression/incorporation of mutant protein. Therefore analysis of mutant protein in the contractile apparatus is necessary. Myosin was extracted from fiber bundles of soleus muscle biopsies by a modified Hasselbach-Schneider solution and digested by endoproteinase Lys-C. The resulting peptide mixture was fractionated by HPLC. The wild type fragment including position 606 exhibits a M_r = 1476, whereas that of the mutation 606 Val→Met a M_r = 1507. The fractions containing these peptides where analysed by matrix assisted laser desorption/ionization mass spectrometry (MALDI-MS) and by electrospray ionization mass spectrometry (ESI-MS).The amino acid sequences of the peptides were determined by collision-activated dissociation (MS/MS).The amino acid sequences obtained confirm the presence of mutated myosin in soleus muscle even from the asymptomatic patient. Mass spectrometry in combination with HPLC thus provides a rather rapid and reliable method for the detection of mutated proteins. We are currently improving this new method to quantify the incorporation of mutated myosin. Varying ratios of mutated to wild type protein incorporated into the muscle fibers may explain the differences in symptoms between patients with FHC as well as differences in physiological parameters between muscle fibers from these patients.

Th-AM-F5

DEFINING A REGION WHICH LINKS STRUCTURAL AND KINETIC CHANGES IN SMOOTH MUSCLE MYOSIN. ((**Rodney A. Brundage**[+], Elizabeth M. Wilson-Kubalek[||], Michael Whittaker[||] Ronald A. Milligan[||], Charles P. Emerson Jr.[#], and H. Lee Sweeney[*])). Departments of Physiology[+*] and Cell and Developmental Biology[+#], University of Pennsylvania; Department of Cell Biology[||], The Scripps Research Institute.

The genetic structure and the muscle specific expression of alternative exon combinations from the single, complex *Drosophila melanogaster* muscle myosin gene provide a potential "blueprint" for tailoring myosin function to muscle type in *Drosophila*. To ascertain the functional consequences of this strategy, we have created and analyzed the structural and kinetic properties of chimeric smooth muscle myosin proteins containing regions of alternative amino acids found within the *Drosophila* gene. As recently described, smooth muscle myosin, unlike skeletal muscle myosin, pivots through a substantial angle between the MgADP bound and rigor (nucleotide free) states when bound to actin. Substitution of a small alternative *Drosophila* exon sequence greatly reduces the rotation of smooth muscle myosin which is associated with MgADP release. In addition, this substitution increases the rate of MgADP release as measured by stopped flow kinetics by 3x (from 90/sec to 270/sec). Substitution of another alternative sequence did not alter the kinetics of MgADP release by smooth muscle myosin. We will present three-dimensional maps of S1-decorated F-actin, in the presence and absence of MgADP, and kinetic data including MgADP release and actin activated ATPase parameters for both chimeric proteins. Our preliminary data suggest that the genetic structure of *Drosophila* muscle myosin provides a novel way to modulate the structural and kinetic features of myosin via alterations in a small region of the protein.

Th-AM-F6

THE ROLE OF A NONCONSERVED SURFACE LOOP IN MYOSIN FUNCTION. ((**C.T. Murphy** and J.A. Spudich)) Dept. of Biochemistry, Stanford University, Stanford, CA 94305

While most of the motor domain of myosin is highly conserved among various organisms and tissue types, the junctions between the 25-kDa and 50-kDa domains ("Loop 1") and the 50-kDa and 20-kDa domains ("Loop 2") are strikingly divergent. It is possible that the lack of conservation in these regions merely reflects a lack of functional constraints. It is also plausible, however, that these regions are capable of modulating the rates of myosin's enzymatic activities. Loop 2 is positioned to modulate actin interactions, while Loop 1 is situated near the ATP binding site (Rayment et al., *Science* **261**: 50, 1993). Loop 2 of *Dictyostelium discoideum* myosin II was substituted with loops from conventional myosins of other organisms (Uyeda et al., *Nature* **368**: 567, 1994); the actin-activated Mg^{2+}-ATPase activities of the chimeras were shown to correspond with the ATPase rates of the donor myosins. We have taken a similar approach to study the role of Loop 1 by making chimeras containing the *Dictyostelium* myosin heavy chain with Loop 1 from two enzymatically diverse myosins, rabbit skeletal (R11) and *Acanthamoeba* (A11). Both chimeras develop normally and are capable of cytokinesis in suspension, and their actin-activated ATPase activities are close to wild type. In contrast, R11's *in vitro* motility is similar to wild-type myosin motility, while A11 moves at about one-third the speed of wild-type myosin. Solution ATPases and stopped-flow spectrophotometry studies with the S1 forms of these chimeras are underway. An understanding of the role of these loops in myosin function may serve as a model for the function of nonconserved surface loops in other proteins.

Th-AM-F7

A UNIQUE DOMAIN IN THE ACTIN-BINDING LOOP (ABL) IS REQUIRED FOR PROPER REGULATION OF SMOOTH MUSCLE MYOSIN. ((**A.S. Rovner**)) Dept. Molecular Physiology & Biophysics, Univ. of Vermont Col. of Medicine, Burlington, VT 05405-0068. (Spon. by J.N. Peterson)

Recently, we used the baculovirus system to show that chimeric substitution of the ABL from chicken skeletal muscle myosin for the endogenous ABL of gizzard smooth muscle myosin caused activation of the de-phosphorylated molecule (Rovner et al., J. Biol. Chem. **270(51)**: 30260-30263). The ABL sequence in the chimeric mutant (named **SABL**) is 12 residues shorter than the smooth ABL, and lacks a highly-conserved sequence domain found in a number of myosins (including smooth) which are regulated by phosphorylation of the regulatory light chain (RLC). To determine whether this domain is responsible for the inhibition of smooth muscle myosin activity in the de-phosphorylated state, recombinant molecules were expressed in which the domain was either subtracted from the smooth muscle loop (**ABL-12**) or added to the sequence of the skeletal loop in the SABL mutant (**SABL+12**). Actin-activated ATPase assays show that deletion of the putative inhibitory domain significantly increases the activity of both phosphorylated and de-phosphorylated ABL-12 relative to the expressed wild-type control, producing a molecule which is poorly regulated by RLC phosphorylation. Conversely, addition of the domain to the SABL mutant to form SABL+12 inhibits activity, producing a molecule with regulatory characteristics very similar to the wild type molecule. Analysis of unloaded actin filament motility *in vitro* shows that ABL-12 moves filaments in the absence of RLC phosphorylation, while SABL+12 does not, confirming that the inhibitory domain is required for proper regulation of the molecule. These results highlight the importance of structural variation in this flexible loop by showing that it affects both the activity and regulatory properties of the myosin molecule.

Th-AM-F8

ANALYSIS OF STRUCTURAL FACTORS INFLUENCING "BACK DOOR" Pi RELEASE IN MYOSIN ((J. David Lawson*, Ralph G. Yount*, and Ivan Rayment†)) *Dept. of Biochem. and Biophy., Washington State Univ., Pullman, WA 99164. †Dept. of Biochem. and Inst. for Enzyme Research, Univ. Wisconsin, Madison, WI, 53705.

The "back door" is a putative secondary entrance/exit to the active site in myosin. Because the back door is only partially open in the x-ray crystal structures, this project was undertaken to determine if it is plausible for the cleaved Pi of ATP to exit the active site via the back door in these structures. Molecular dynamics simulations were performed on the active site/back door region of the S1Dc•MgADP•BeF_x crystal structure (Fisher et al. 1995. *Biochemistry 34*: 8960-72) in which BeF_x was replaced with Pi. The first simulation examines the "breathing" of the phosphate tube (a solvent filled passage leading from the binding site of the γ-phosphate to the back door). Our simulation indicates that thermal motions of the side chains along the phosphate tube are sufficient to expand its approximate diameter from ~3.8 Å in the crystal structure to as large as ~9.5 Å. This is likely large enough to allow the ~6.0 Å diameter Pi to pass through. The second simulation uses a spring constant to pull Pi down the phosphate tube towards the back door opening. In a 50 ps simulation, Pi is pulled ~4 Å down the phosphate tube towards the back door opening thus demonstrating that side chains lining the phosphate tube have enough freedom of movement to permit the passage of Pi. Furthermore, analysis of the S1Dc•MgADP•Vi structure, (Smith and Rayment. 1996. *Biochemistry 35* 5404-17) reveals that the partial closure of the 50 kDa cleft collapses the phosphate tube and thus blocks the back door. These observations suggest that the ability of Pi to leave via the back door is controlled by both contractile cycle conformational changes and by thermal motions of side chains in the active site/back door region. This work was supported by NIH grants DK05195 (RGY) and AR35186 (IR) and by a NIH Biotechnology Training grant GM08336 (JDL).

Th-AM-F9

DIRECT OBSERVATION OF SEGMENTAL FLEXIBILITY IN MYOSIN HEADS. ((**S. A. Burgess**, M. Walker, H. White, J. Trinick)) Veterinary School, Bristol University, Langford, Bristol, BS18 7DY, U.K & Eastern Virginia Medical School, Norfolk, VA 23507.

Electron microscopy of negatively stained myosin reveals three discrete regions within the head parts of the molecule; these correspond to the motor domain and the essential and regulatory light chains. In this study, we applied single-particle analysis using the SPIDER software, combining individual head images from molecules prepared in the absence of nucleotide and classifying them into homogeneous groups. The improved signal-to-noise ratio in these groups resulted in substantially improved detail. The primary data set consisted of 2289 aligned heads. Initial attempts to classify the heads into homogeneous groups proved unsuccessful. Although the motor domain had several distinct features and an obvious one-sidedness, the light chains varied in position relative to the motor domain. Classification based solely on the motor domain did produce homogeneous groups and divided the heads into 6 major classes. We compared these class averages to a series of views generated from a simple negative stain model of the atomic structure of myosin-S1. The stain images were broadly consistent with the model and the 6 classes appeared to be related by a rotation about an axis through the long heavy chain -helix of the head, covering an angular range of ~150°. Having established that classification based on the motor domain was meaningful, each group was subjected to a further round of classification, this time based only on the essential and regulatory light chain regions. Each of the 6 groups was found to be composed of sub-classes that retained their characteristic motor domain appearances, but showed variable essential and regulatory light chain dispositions resulting from bending of the head. In four of the groups it was possible to estimate the movement of the regulatory light chain region to be about 4 nm. This work was supported by the MRC and AR40964

K CHANNEL GATING II

Th-AM-G1

FLUORESCENCE MEASUREMENTS OF VOLTAGE-DEPENDENT CHANGES IN THE *SHAKER* POTASSIUM CHANNEL. ((**A. Cha** and F. Bezanilla)) Depts. of Physiology and Anesthesiology, UCLA School of Medicine, Los Angeles, CA 90095.

We are using epifluorescence to examine the conformational changes that are occurring within the *Shaker* potassium channel during voltage-dependent activation. By using cysteine-scanning mutagenesis and labeling expressing *Xenopus* oocytes with TMRM, a rhodamine-based sulfhydryl-reactive probe, we can detect conformational changes in non-conducting *Shaker* K^+ channels (W434F) by simultaneously measuring gating currents and fluorescence changes (ΔF) in a manner similar to that described in Mannuzzu et al., *Science* (1996). We have also developed a method of recording the fluorescence signal using the cut-open oocyte clamp, allowing more detailed kinetic analysis of the components of simultaneously measured gating currents and fluorescence under conditions of spatial voltage uniformity. To date, the S4 mutants M356C, A359C, and R365C yield a fluorescence signal that changes during an applied voltage pulse, indicating a conformational change associated with the S4 segment. However, the S4 mutant V363C appears to be labeled by TMRM but does not show a voltage-dependent fluorescence change. The time scale, direction, and magnitude of the fluorescence changes in the other three mutants do not correlate well with the measured movement of gating charge. The ΔF-V curve measured at 400 ms is significantly steeper than the Q-V curve with a holding potential (HP) of either -90 mV or 0 mV. When pulsing from either HP to the range of -50 to -30 mV, the fluorescence has a very slow component that has no measurable counterpart in the time integral of the gating current. At a HP of 0 mV, the Q-V curve is shifted to more negative potentials than the ΔF-V curve, and it is possible to record large ΔF signals in the virtual absence of gating currents. These results indicate that ΔF measurements may allow the detection of conformational changes that are either too slow to produce a detectable gating current or do not move charge through the field. Supported by NIH grants GM30376 and GM08042.

Th-AM-G2

AN ACTIVATED INTERMEDIATE OF A VOLTAGE-GATED K^+ CHANNEL: *S4 TRANSMEMBRANE TOPOLOGY IN BETWEEN THE RESTING AND OPEN STATES*. ((**O.S. Baker**, H.P. Larsson, L.M. Mannuzzu and E.Y. Isacoff)) Group in Biophysics and Department of Molecular & Cell Biology, UC Berkeley.

Previously, analysis of the kinetics and steady-state voltage dependence of charge movement in Shaker channels has suggested that channel activation involves two, quasi-independent charge-moving steps, "Q_1"and "Q_2" (Bezanilla, *et al*, 1994, Biophys J 66:1011). In wild-type gating Shaker channels these steps closely overlap. We have characterized a mutant channel exhibiting two steps of charge activation, Q_1' and Q_2', that do not overlap. The fully deactivated state, according to the accessibility of a cytosol-facing cysteine "reporter," exhibits S4 topology like that of fully deactivated, wild-type gating Shaker channels. When fully activated, the mutant channels open and exhibit S4 topology like that of open, wild-type gating channels, as assayed by an outside-facing accessibility reporter. At potentials in between those which activate Q_1' and Q_2', however, channel subunits reside predominantly in an intermediate state, in which S4 topology is in between its extreme activated and deactivated positions. Fluorescence changes reported by an S4-coupled probe indicate that Q_1' and Q_2' arise from two stages of S4 movement; which appear to move S4 progressively outward with activation. These results offer insights into what the long postulated intermediate closed states of channels look like. They also argue that S4 movement governs channel activation throughout more than one phase, and suggest that the range of S4 movement may vary within the superfamily of voltage-gated channels, depending, at least in part, on S4 sequence.

Th-AM-G3

SUBUNIT COOPERATIVITY IN *SHAKER* POTASSIUM CHANNEL GATING. ((**L.M. Mannuzzu** and E.Y. Isacoff)) Department of Molecular and Cell Biology, University of California, Berkeley.

Although there is evidence for cooperativity in the activation of *Shaker* channels, it has neither been possible to identify the cooperative steps of activation, nor to quantitate the cooperativity. This requires a method to monitor separately gating movements in individual subunits, and to isolate for study the different phases of activation. We have addressed this problem by taking advantage of the ability of voltage-clamp fluorimetry (VCF; Mannuzzu et al., 1996, Science 271, 213-16) to monitor structural rearrangements in one subunit at a time. We made heteromultimeric channels containing two types of subunits: one with a cysteine in S4, which can be labeled with a fluorophore, allowing monitoring of S4 movement by VCF; and one that would not be labeled, but had a mutation that shifts particular phases of the gating charge movement. The expectation was that, if gating involves cooperativity between subunits, the voltage-shifted subunits would alter the fluorescence-voltage relation (F-V) of the labeled wild-type subunit over a voltage range that triggers those cooperative gating steps. Co-injection in *Xenopus* oocytes of cRNA encoding S352C as the "reporter" subunit, and either wild-type or L382V subunits, in a ratio favoring the unlabelable subunits, resulted in identical F-Vs for 352C homomultimers and heteromultimers of 352C + wild-type, whereas the F-V of the heteromultimers of 352C + L382V was altered in such a way that it closely resembled the F-V of the double mutant 352C/L382V. These results indicate the existence of subunit cooperativity in activation steps leading to and/or including the one altered by the L382V mutation, which has been postulated to be a late cooperative step (Sigworth, 1994, Quart. Rev. Biophysics 27, 1-40). Subunit interactions in other gating transitions are currently under study.

Th-AM-G4

THEORY OF S4-MOTION IN VOLTAGE-GATED CHANNELS.
((**H. Lecar** and H. P. Larsson)) Department of Molecular & Cell Biology, University of California, Berkeley, CA, 94720.

With increasing knowledge of the molecular structure of voltage-gated sodium and potassium ion channels, the membrane-spanning domain S4, posessing a unique string of charged residues has been identified as the likely voltage sensor of the channel protein. Recent experiments on the Shaker K^+ channel (Larsson, Baker, Dhillon and Isacoff, Neuron 16, 387,1996) provide a picture of the outward movement of S4 residues through the membrane interface during gating. We derive the major features of the gating process for wild-type and mutant channels from the statistical mechanics of the S4 subunits moving under the stress of the transmembrane electric field. The potential energy function for the translocation of the S4 gating charges is dominated by the coulomb interaction between the S4 charges and nearby counter charges on neighboring helices, the image potential for charge groups which move through the membrane-solution interface, and the work done by the external field in moving the charges across the membrane. We show how the superposition of these rather long-range potentials can lead to an energy-well pattern giving a small number of deep energy minima, which correspond to the stable states of a simple reaction-kinetic scheme. The calculations from 'first principles' predict energies and charge displacements which account for the gating charge relations observed for the K^+ channel and the variations observed for various mutants in which the charge structure is altered.

Th-AM-G5

PHOSPHORYLATION AT MULTIPLE N-TERMINAL SITES DIRECTLY MODULATES INACTIVATION OF Kv3.4. ((**M. Covarrubias**, E.J. Beck, A. Matlapudi and R. G. Sorensen)). Dept. of Pathology, Anatomy and Cell Biology, Jefferson Medical College, Philadelphia, PA.

In a previous study we reported that protein kinase C (PKC) eliminates rapid inactivation of A-type K^+ channels encoded by Kv3.4 (Neuron, 13:1403-1412, 1994). This effect is due to phosphorylation of Ser^8, Ser^9, Ser^{15} and Ser^{21}. To investigate whether impaired inactivation can be explained by the electrostatic effect of added phosphate groups, we created a series of mutant channels in which Asp (a negatively charged amino acid) was substituted for Ser either alone, or in various combinations (Ser^8>Asp, Ser^9>Asp, Ser^{15}>Asp, Ser^{21}>Asp, double, triple and quadruple mutants). Clearly, the effect of PKC on Kv3.4 inactivation was mimicked by these mutations (Fig. 1). In agreement with electrophysiological and biochemical experiments, we also found that residues at positions 8 and 9 are especially critical. Supported by NIH grants NS32337 (M.C.) and NS31670 (R.G.S.).

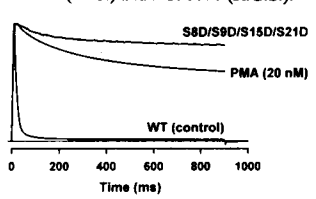

Figure. 1. Normalized whole-oocyte currents elicited by a step depolarization to +50 mV (Vh= -100 mV). Wild-type was recorded in the absence (control) and presence of a phorbol ester (PMA). Quadruple mutant was recorded in the absence of PMA.

Th-AM-G6

CONSERVATIVE SUBSTITUTIONS AT NONCHARGED RESIDUES IN S4 THAT SLOW A COOPERATIVE TRANSITION IN THE ACTIVATION PATHWAY GREATLY ALTER VOLTAGE-DEPENDENCE OF GATING Jennifer Ledwell, Cathy Smith-Maxwell, and Richard W. Aldrich, Dept. of Molecular and Cellular Physiology and Howard Hughes Medical Institute, Stanford University, Stanford, CA 94305.

We have been studying the relationship between gating charge movement and the voltage-dependence of ionic currents in two mutants in a Shaker background. Shaw S4 is a chimera in which the S4 sequence of the *Drosophila* channel, *Shaw*, has been subsituted into Shaker. This substitution shifts the mid-point of the conductance-voltage relationship by +121 mV and decreases the slope of this curve by a factor of three. The time course of activation is slower than that of Shaker and is well-described by a single exponential function, indicating the prescence of a rate-limiting, cooperative step in the activation pathway. The second mutant, ILT, has only three of the eleven amino acid substitutions present in Shaw S4. Together, these three conservative substitutions (V369I, I372L, S376T) can reproduce the basic features of the conductance-voltage relationship and kinetics of the ionic currents of Shaw S4. We have measured gating currents for ILT and have found that, although channels open at voltages between 20 to 200 mV, approximately 90% of the gating charge moves between -120 and -40 mV and has rapid kinetics similar to Shaker. A smaller component of gating current (10% of total) can be observed in the more positive voltage range where channels open. The gating current results suggest that the activation pathway for ILT resembles that of Shaker except for a rate-limiting, highly cooperative conformational change late in the activation pathway. The dramatically altered voltage-dependence of the ionic currents is the result of this slowed, cooperative step in the activation pathway. Preliminary experiments on Shaw S4 indicate that Shaw S4 and ILT do not have similar gating currents despite the similarity of their ionic currents.

Th-AM-G7

CHEMICAL MODIFICATION OF HISTIDINE 404 IN KV1.3 INCREASES THE RATE OF CHANNEL INACTIVATION AND SENSITIVITY TO EXTRACELLULAR POTASSIUM.
((**Linda D. McCauley**, Angela Nguyen, and Michael D. Cahalan)) Department of Physiology and Biophysics, University of California, Irvine, CA 92697.

Histidine 404 of the voltage-gated K^+ channel Kv1.3 plays a critical role in determining channel properties such as C-type inactivation and sensitivity to extracellular TEA and toxins. We have studied the effect of diethylpyrocarbonate (DEPC), a histidine specific reagent, on rat basophilic leukemia (RBL) cells microinjected with Kv1.3 cRNA. Cells were patch-clamped in normal mammalian Ringer (pH 7.4) and held at -80 mV. DEPC dissolved in Ringer at pH 6 was applied for 1.5 min while the channels were closed. Inactivation time constants during prolonged depolarizations were almost 2-fold faster following DEPC treatment. The removal of extracellular potassium in control experiments resulted in a 64% reduction in conductance. In DEPC-modified channels the reduction was increased to 80%. To confirm the specificity of this reaction, similar experiments were performed on cells injected with valine replacing the H404. Cells expressing the H404V mutant channels were not susceptible to DEPC modification. These results suggest that H404 is accessible in the closed state and underscore the importance of position 404 in determining Kv1.3 channel properties. Supported by grant NS 14609.

Th-AM-G8

A NOVEL MECHANISM OF INACTIVATION IN SHAL K^+ CHANNELS. ((**H.H. Jerng** and M. Covarrubias)) Dept. of Pathology, Anatomy and Cell Biology, Jefferson Medical College, Philadelphia, PA 19107.

We have investigated the mechanism of rapid inactivation of a Shal K^+ channel (mKv4.1) expressed in Xenopus oocytes. The inactivation gate of mKv4.1 does not seem to behave like an open-channel blocker because a high external $[K^+]$ (98mM) slowed down recovery from inactivation (τ_{rec} @ -80mV: 400 ms and 660 ms in 2mM and 98mM $[K+]_e$, respectively). Moreover, exposure to 5mM internal TEA inhibited peak current by ~60% but failed to slow down rapid inactivation and neutralization of N-terminal residues (R13, R34, and K37) by site-directed mutagenesis had no effect on inactivation. On the other hand, exposure to 98mM external TEA inhibited peak current by ~30% but also failed to slow down inactivation. These results suggested that mKv4.1 inactivates by a mechanism that appears distinct from N-type or C-type inactivation as known in Shaker K^+ channels. The study of N- and C-terminal deletion mutants revealed that rapid inactivation of mKv4.1 is mediated by elements within both the hydrophilic N- and C-terminal domains (Jerng and Covarrubias, Biophys. J., in press), and suggested that the termini may interact to maintain the N-terminal inactivation gate near the inner mouth of the pore. In dominant suppression experiments, we co-expressed mKv4.1 and various N- and C-terminal deletion mutants with a peptide corresponding to the first 62 residues of mKv4.1 (N62). N62 reduced currents mediated by mKv4.1 WT (~85%), Δ2-72 (~95%), and Δ494-651 (~80%). However, N62 had no effect on Δ422-651, a mutant that removed 230 residues at the C-terminus. We hypothesize that the distal N-terminal region may interact with a highly basic C-terminal domain proximal to S6. Supported by NIH grant NS32337 (M.C.) and training grant AA07463.

Th-AM-G9

GATING KINETICS OF HERG K+ CHANNELS IS DETERMINED BY THE N-TERMINAL DOMAIN AND PROTEIN PHOSPHORYLATION.

((**R. Schönherr**, R. Meyer, Y. Kubo* and S.H. Heinemann)) Max-Planck-Gesellschaft, AG Molekulare & zelluläre Biophysik, Jena, Germany, *Tokyo Metropolitan Insitute for Neuroscience, Tokyo, Japan.

HERG has recently been identified as the locus for an inherited form of the long QT syndrome (LQT2), a cardiac disturbance with the risk of sudden death. Upon expression in *Xenopus* oocytes HERG behaves as a depolarization-dependent inward rectifier channel, which is characterized by fast C-type inactivation and slow deactivation. As the main current flow occurs after recovery from inactivation, the speed of deactivation is limiting for HERG currents. The deactivation kinetics is strongly accelerated upon complete deletion of the N-terminal domain (Schönherr & Heinemann, 1996, J. Physiol. 493:635). The detailed analysis of further N-terminal deletion constructs (Δ2-15, Δ2-109, Δ2-218) revealed that the first 15 residues are required for slow deactivation. All deletions lead to fast deactivation; at -120 mV the construct lacking residues 2 to 15 showed a deactivation time constant (τ_d = 13±2.6 ms, n=12) about 8 times faster than the wild-type (τ_d = 108±15 ms, n=7). A point mutation within the first 15 residues (Q11K) also resulted in accelerated deactivation (τ_d = 31±6 ms, n=8). As a general observation we found that HERG deactivation varied with different batches of oocytes used for expression. To see whether HERG gating can be modulated by the cells, we coexpressed the channel with the gonadotropin releasing hormone receptor. Upon addition of the activating peptide, HERG channels responded with an acceleration of the deactivation process. The same effect could be induced by application of diacylglycerol to the oocytes, suggesting that protein kinase C must be involved in the regulatory process.

LOCAL CALCIUM TRANSIENTS: CARDIAC MUSCLE

Th-AM-H1

SR RELEASE FLUX UNDERLYING Ca^{2+} SPARKS IN CARDIAC MUSCLE

((**Lothar A. Blatter**[1], Jörg Hüser[1] and Eduardo Ríos[2])) [1]Department of Physiology, Loyola University Chicago, Maywood, IL 60153, and [2]Department of Molecular Biophysics and Physiology, Rush University, Chicago, IL60612.

Contraction of cardiac muscle requires release of Ca^{2+} from the sarcoplasmic reticulum (SR) through ryanodine receptors by Ca^{2+}-induced Ca^{2+} release. Discrete events of SR Ca^{2+} release (Ca^{2+} sparks) observed in atrial and ventricular myocytes have been proposed to represent elementary events of cardiac SR Ca^{2+} release. It remains a question of debate, however, whether Ca^{2+} sparks originate from single release channels or multiple channels clustered in close vicinity. Generalizing methods used earlier to describe cell-averaged Ca^{2+} release we have calculated from confocal line scan images the flux of Ca^{2+} release underlying Ca^{2+} sparks as a function of space and time. Analysis of spontaneous sparks recorded from single cat atrial myocytes revealed in most cases single sparks of Ca^{2+} release originating from 1 μm wide regions. The estimated release flux amounts to approximately 15 mM/s at the peak, which corresponds to a flux of 1.5 x 10^{-17} mole/s of Ca^{2+} ions, or 3 pA. In many cases doublets and triplets of release sparks were observed. The spacing between individual release sparks within multiplets was 0.3-0.8 μm. If each release spark in a multiplet originates from one 'peripheral coupling' (cluster of Ca^{2+} release channels associated with the sarcolemmal membrane), then the activation is capable of rapid propagation between couplings, over distances ≥ 0.5 μm. This indicates that propagation should also occur between neighboring channels within a junction (≈ 30 nm apart). Therefore we propose that cardiac Ca^{2+} sparks originate from concerted opening of multiple channels within discrete functional and morphological SR units. (supported by NIH, AHA, MDA, Schweppe Fdn.).

Th-AM-H2

CA^{2+} SPARKS TRIGGERED BY L-TYPE CA^{2+} CURRENTS CAN INVOLVE MULTIPLE SITES.

((W.J. Zang, I. Parker, C.W. Balke and W.G. Wier)) University of MD at Balt., 655 W. Baltimore St. Baltimore, MD 21201.

Calcium (Ca^{2+}) sparks are localized calcium transients occurring at rest and during depolarization in cardiac muscle cells. Our previous work, using confocal line-scan imaging, has shown that spontaneous calcium sparks arise at sites spaced regularly in the *longitudinal* direction of the cell's axis, at intervals of 1.8 μm (i.e. reflecting the longitudinal distance between 'Z' lines), but are packed closely and irregularly in *transverse* planes along Z lines (mean transverse spacing between sites of 0.76 μm). Furthermore, line-scan confocal imaging in the transverse direction of the cell axis revealed that spontaneous Ca^{2+} sparks often involve multiple, closely spaced sites of release at a single Z line. The present study was undertaken to determine whether or not calcium sparks triggered by L-type Ca^{2+} channel currents also involve multiple sites of release. During voltage-clamp pulses to -30 mV, individual evoked Ca^{2+} sparks could be observed. With transverse scanning, fifty one (51) percent of the evoked sparks had multiple sites of origin. With longitudinal scanning only a few (< 2%) had multiples sites of origin. In transverse scans the distance between sites ranged between 0.5 μm (the minimum that can be resolved) and 1.2 μm. Thus, Ca^{2+} sparks evoked by the Ca^{2+} entering via L-type Ca^{2+} channels are not always elementary' events, in the sense of being indivisible, but can be comprised of triggered units of Ca^{2+}release. Support: HL55280 (W.G.W.), HL50435 (C.W.B.) and GM48071 (I.P.).

Th-AM-H3

NEAR-MEMBRANE DETECTION OF CA^{2+} IN CARDIAC MYOCYTES

((L. A. Blatter* and E. Niggli*)) Depts. Physiology, *University of Bern, Bern, Switzerland, [1]Loyola University, Chicago (spon. by J. S. Shiner)

Near-membrane [Ca] may differ significantly from bulk cytosolic [Ca], particularly during rapid Ca signalling events related to cardiac muscle ec-coupling. We used the lipophilic membrane-associated Ca indicator Ca-Green C-18 (C-18) and laser-scanning confocal microscopy to detect changes of t-tubular and extracellular [Ca] in cultured neonatal rat myocytes and in freshly isolated guinea-pig ventricular myocytes. Changes of extracellular [Ca] were readily detected by the C-18 located in the cell membrane. Control experiments were carried out with 100 mM extracellular Ni to rapidly quench the fluorescent indicator accessible form the extracellular space. Ni quenched C-18 fluorescence to levels below F_{min} indicating that C-18 was located in the outer leaflet of the cell membrane. In contrast, the lipophilic derivative of Indo-1 (FIP-18) was significantly internalized, as visualized using two-photon excitation of FIP-18. Surprisingly, in low extracellular [Ca] C-18 located in the outer leaflet of the cell membrane also reported transient elevations of intracellular [Ca] during application of 10 mM caffeine. In the absence of extracellular Na to inhibit Ca removal via Na-Ca exchange, the intracellular Ca signals evoked by caffeine were prolonged, as recorded with Fura-Red. However, the near-membrane Ca signal simultaneously detected by C-18 did not increase during caffeine stimulation in the absence of extracellular Na. These results suggest that the C-18 signal reports extrusion of cytosolic Ca from the subsarcolemmal space mediated by Na-Ca exchange. (Supported by SNF and Schweppe Foundation Chicago).

Th-AM-H4

CALCIUM ENTRY THROUGH L-TYPE CALCIUM CHANNELS DIRECTLY TRIGGERS CALCIUM SPARKS.

((**S.R. Shorofsky**, L.T. Izu, W.G. Wier, C.W. Balke))University of Maryland, Baltimore, MD 21201

The local control hypothesis predicts that calcium entry through L-type Ca^{2+} channels causes release of Ca^{2+} from the junctional SR in the immediate vicinity of the channel. To test this hypothesis directly, we measured the occurrence of Ca^{2+} sparks using laser-scanning confocal microscopy just beneath the tip of an on-cell patch clamp electrode under experimental conditions where only L-type Ca^{2+} channels are activated. The pipette solution contained 10 mM Ca^{2+} with TTX and TEA to block Na^+ and K^+ channels, respectively. Bay K8644 and isoproterenol were added to increase the probability of channel opening and their duration. Voltage clamp protocols entailed 90mV depolarizations from the resting potential. Line scans images(500Hz scan rate) were obtained for 300 msec before and after each voltage step. Twenty-two cells from eleven animals were studied. **Results:** There was a 35% increase in the probability of observing a Ca^{2+} spark following the voltage step within a 4μm area centered on the pipette tip (3.5% vs 2.6%,$p<0.05$). The probability of observing a Ca^{2+} spark 20μm from the pipette was 1.7% per sweep and unaffected by the voltage step. When Ca^{2+} in the pipette was replaced with Ba^{2+}, there was no increase in Ca^{2+} spark probability following a voltage step despite observing openings of L-type Ca^{2+} channels. **Conclusion:** These results demonstrate that Ca^{2+} entry through a limited number of L-type Ca^{2+} channels causes the release of Ca^{2+} from the SR immediately beneath the membrane patch.

Th-AM-H5

ACTIVATION OF Ca^{2+} BUFFERED HEART CELLS BY STRINGS OF Ca^{2+} SPARKS.

((L. Cleemann, W. Wang and M. Morad)). Department of Pharmacology. Georgetown University Medical Center. Washington, DC 20007.

Intracellular calcium movements were imaged in voltage clamped rat ventricular myocytes at a frame rate of 120 Hz using a rapidly scanning, confocal, fluorescence microscope (Noran, 100 ns per pixel). The cells were dialyzed with fluorescent Ca^{2+}-probe (1 mM Fluo-3) and 5-10 mM EGTA to lower the resting Ca^{2+} concentration (<50 nM) and reduce the magnitude of caffeine- and I_{Ca}-induced intracellular Ca^{2+}-transients (<120 nM) without suppressing the total release (≅140 μM) (Adachi-Akahane et al. 1996, J. Gen. Physiol. vol. 108). The two Ca^{2+} buffers together reduce the diffusion distance of released Ca^{2+} (to <50nm) and act in tandem to briefly register the released Ca^{2+} with Fluo-3 but quench longer lasting fluorescence signals with EGTA. At -70 mV holding potentials Ca^{2+} sparks occurred at a low frequency with maximal intensity lasting about one frame 8 ms. They were visualized as bright circular spots (< 1 μm) at sites conforming to the sarcomere pattern. In the following frame the sparks generally faded 50 to 80% and spread over a distance of 2 to 3 μm. Occasionally dual sparks were seen as jumping either in the direction of the z-line or from one sarcomere to the next. Voltage clamp depolarization produced a characteristic fluorescence pattern of randomly beaded ridges. Sites of repeated Ca^{2+} release were identified with better than 0.5 μm resolution during repeated depolarization, and produced a cumulative pattern of ridges showing both striation and myofibrils. In single frames the rate of ongoing release was estimated by integrating the fluorescence intensity along the ridges and subtracting the integral intensity from that of in between valleys. This measure allowed the rate of Ca^{2+} release to be followed during voltage clamp pulses and be correlated to the time course of the Ca^{2+} current and its tail transient. These measurements suggest that the combination of fluorescent and non-fluorescent Ca^{2+} buffers in millimolar concentrations may improve spatial and temporal resolution of Ca^{2+} measurements and allow direct visualization of μ-domains with Ca^{2+}-induced Ca^{2+} release during activation of mammalian heart cells. *Supported by NIH HL16152.*

Th-AM-H6

CALCIUM SPARKS IN SPONTANEOUSLY HYPERTENSIVE RATS WITH CARDIAC HYPERTROPHY

((S.R. Shorofsky, W.G. Wier, **C.W. Balke**)) University of Maryland School of Medicine, Baltimore, MD, 21201.

The specific abnormalities in intracellular Ca^{2+} regulation that occur with cardiac hypertrophy remain unknown despite extensive investigations. In this study, we applied confocal microscopy to study Ca^{2+}-sparks (i.e. local SR Ca^{2+}-release) in ventricular myocytes from spontaneously hypertensive rats (SHR) with mild hypertrophy (4-6 month old) and age-matched control rats. Freshly isolated cells were loaded with fluo-3 AM and imaged using a laser scanning confocal microscope in the line scan mode. Spontaneous and evoked (in the presence of nifedipine) Ca^{2+}-sparks were analyzed (SHR:400; control:244). The SHR had hypertension (151±11 vs 117±12 mmHg) and mild cardiac hypertrophy by heart wt/body wt ratio (6.0±0.8 vs 5.7±1) and cell size (220±41 vs 171±31pF) when compared to control animals. SHR Ca^{2+}-sparks had larger mean amplitudes (161±200 vs 92±49 nM; p<0.001) and larger spreads in their spatial/temporal "areas" (153±120 vs 125±106 pixels; p<0.01). Multiple populations of Ca^{2+}-sparks were observed in both SHR and control with the increase in Ca^{2+}-spark amplitude in SHR due primarily to an increase in the number of Ca^{2+}-sparks of the largest amplitude. We conclude 1) that multiple populations of Ca^{2+}-sparks exist in both normal and SHR, possibly representing the recruitment of additional SR Ca^{2+}-release units, and 2) that the increased proportion of SHR Ca^{2+}-sparks of higher amplitude may explain some of the important changes in contractility seen with cardiac hypertrophy.

Th-AM-H7

ARTIFICAL Ca^{2+} SPARKS BY DIFFRACTION-LIMITED TWO-PHOTON PHOTOLYSIS

((P.Lipp, C.Lüscher, C.Amstutz and E.Niggli)) Dept. Physiology, University of Bern, Switzerland

In cardiac muscle the action potential of the cell membrane is transduced into the mechanical activity by Ca^{2+}-induced Ca^{2+}-release (CICR) from the sarcoplasmic reticulum (SR). Cardiac Ca^{2+} signalling follows a hierarchical concept, whereby the Ca^{2+} quark (arising from single-channel gating of a ryanodine receptor) and the Ca^{2+} spark (caused by concerted recruitment of Ca^{2+} quarks) are the elementary building blocks for cellular Ca^{2+} transients. Ca^{2+} sparks show-up as spatially restricted Ca^{2+}-release transients, either spontaneously or triggered by L-type Ca^{2+} channels. In this study we addressed the question, whether highly confined photolysis of caged Ca^{2+} can trigger SR-Ca^{2+} release. A two-photon (TP) excitation laser system was combined with a laser-scanning confocal microscope in order to follow the subcellular Ca^{2+} transients. Cardiac myocytes were patch-clamped and dialyzed with an internal pipette solution containing 1mM DM-nitrophen (preloaded with 0.25 mM $CaCl_2$) and 0.1 mM Fluo-3. Initial experiments were performed in droplets of pipette solution, whereby TP-excitation was confined to a diffraction limited volume. TP-photolysis of DM-nitrophen was obtained at 710 nm (repetition-rate: 76 MHz; pulse-duration ≈ 80 fs). Under these experimental conditions, the photolytic Ca^{2+} transient was smoothly graded with the input average energy (10 to 100 mW). Diffraction-limited point-photolysis of DM-nitrophen in single cardiac myocytes evoked subcellularly restricted Ca^{2+} transients at low output energies when illumination was brief. These "artifical Ca^{2+} sparks" had amplitudes between 30 and 300 nM and radial spreading was restricted to 1-5 μm. Increasing either the duration or the illumination energy enabled us to evoke Ca^{2+} release signals that propagated through the myocyte as a Ca^{2+} wave. These results clearly indicate that diffraction-limited TP photolysis is able to trigger SR-Ca^{2+} release by the CICR mechanism. (Supported by SNF)

Th-AM-H8

IDENTIFICATION OF THE HIERARCHICAL Ca^{2+}-SIGNALLING SYSTEM IN NON-EXCITABLE CELLS

((M.Bootman[2], E.Niggli[1], M.Berridge[2] & P.Lipp[1])) [1]Department of Physiology, University of Bern, Switzerland; [2]The Babraham Institute Laboratory for Molecular Signalling, Univ of Cambridge, UK.

Histamine stimulation of HeLa cells evokes cellular Ca^{2+} release from the endoplasmic reticulum by the phosphoinositide pathway. The resulting Ca^{2+} transients are visible as Ca^{2+} spikes and Ca^{2+} waves. We investigated the Ca^{2+} signalling system in this prototype non-excitable cell, in order to identify the elementary building blocks of this transduction pathway. Subcellular Ca^{2+} release signals arising from the gating of inositol 1,4,5-trisphosphate receptors ($InsP_3Rs$) in Fluo3-loaded HeLa cells were visualized using confocal microscopy. Stimulation of cells with Ca^{2+}-mobilizing hormones evoked two distinct populations of subcellular Ca^{2+} signals. "Ca^{2+} blips" ($t_{upstroke}$≈12 ms; spreading ≈ 1.3 μm; amplitude ≈30 nM) were identified as resulting from single-channel gating of individual $InsP_3Rs$ (ionic current ≈ 1 pA), while "Ca^{2+} puffs" ($t_{upstroke}$≈50 ms; spreading ≈ 4 μm; amplitude ≈ 170 nM) resulted from the equivalent gating of approx. 25 $InsP_3Rs$ (ionic current ≈ 25 pA). Both Ca^{2+} signals, blips and puffs, were elementary events responsible for the initiation of homogeneous Ca^{2+} transients and propagating Ca^{2+} waves. We propose that a hierarchical Ca^{2+} signalling system underlies non-excitable cell Ca^{2+} signal transduction, in which the recruitment of elementary events is the basic mechanism to build-up subcellular and cellular Ca^{2+} transients. The hierarchy of Ca^{2+} signalling events identified in HeLa cells, from fundamental (blips) to intermediate (puffs) to global Ca^{2+} signals (e.g. waves), is analogous to the Ca^{2+} quarks, Ca^{2+} sparks and Ca^{2+} waves proposed for cardiac muscle cells.

Th-AM-H9

Ca^{2+} Imaging with a Fast Scanning Confocal Microscope During the Action Potential in Smooth Muscle Cells. Y. Imaizumi, Y. Torii, Y. Ooi, K. Muraki, T.B. Bolton and M. Watanabe, Departments of Chemical Pharmacology, Nagoya City University, Nagoya, Japan and Department of Pharmacology & Clinical Pharmacology, St. George's Hospital Medical School, London, UK (Sponsored by W. Giles)

Ca^{2+} images in single smooth muscle cells were obtained using a fast scanning confocal microscope (Nikon RCM 8000). Smooth muscle cells were isolated from vas deferens or urinary bladder of the guinea-pig. Cells were loaded with 100 μM fluo-3 by diffusion from the recording pipettes used for whole-cell voltage clamp. An image of 170x27.5 μm area (512x128 pixels) was taken every 8 ms. When a cell was depolarized from -60 to 0 mV, an inward Ca^{2+} current, as well as a large transient and smaller sustained outward current were recorded. The large transient outward current which reached a peak at about 20 ms from the start of depolarization was mainly due to activation of iberiotoxin-sensitive Ca^{2+} - dependent K^+ current ($I_{K\text{-}Ca}$). Following each depolarization, the fluorescence intensity started to increase within 5 ms in several small spots located close to the cell membrane (< 1 μm). The increase in intensity in these Ca^{2+} hot spots occurred with a very similar time course to that of $I_{K\text{-}Ca}$ activation. The fluorescent intensity in other cell areas increased far more slowly. Subsarcolemmal hot spots were also observed immediately after an action potential was elicited in current clamp mode. Both hot spots and $I_{K\text{-}Ca}$ were markedly reduced by 10 μM cyclopiazonic acid. These results suggest that during an action potential in these cells rapid Ca^{2+} release from local storage sites is involved in the activation of hot spots and $I_{K\text{-}Ca}$.

Th-AM-I1

GENE V PROTEIN - DNA INTERACTIONS

((C.A. **Edwards**[1], S.V. Santhana Mariappan[2], C.-S. Tung[2] and T.C. Terwilliger[1])) [1] Structural Biology and [2]Theoretical Biology and Biophysics, Los Alamos National Laboratory, Los Alamos, NM 87545. (Sponsor: C.A. Edwards)

Interactions between the aromatic amino acids of Y41H gene V protein and single-stranded oligonucleotides of 4 , 8 and 16 nucleotides in length were investigated using 1D and 2D ^{1}H NMR spectroscopy. Single-stranded nucleic acid binding proteins play roles in key cellular processes including DNA replication, recombination and control of RNA translation. Stoichiometry of 4 protein monomers / 1 16-mer DNA was determined in a fluorescence titration experiment under the conditions used for NMR spectroscopy. 1D proton, TOCSY and NOESY spectra were recorded for DNA, protein and the protein-DNA complex. Upon titration of 16-mer DNA into Y41H gene V protein, the signal from His41, thought to be important in interdimer interactions in DNA binding, is selectively broadened, while no broadening is observed with the 4-mer. Comparison of NOESY and TOCSY spectra recorded for the stoichiometric complex of Y41H gene V protein-4-mer DNA shows changes in chemical shifts for the resonances from Tyr 26 and Phe 73 from those in the protein alone. NOEs were detected between Tyr26 and T2 and between Phe73 and G1, T2 and T3. Also, intramolecular NOEs from DNA in the complex which are not present for free DNA in solution indicate a comparatively rigid placement of DNA on the protein and changes in protein-protein interactions on complex formation compared to free protein suggest rotation of one dimer with respect to the other dimer. Similar interactions are seen in the Y41H-8-mer and Y41H-16-mer DNA complexes.

Th-AM-I2

CD OF FIVE CLASS I FILAMENTOUS SINGLE-STRANDED DNA PHAGES.

((Loren A. Day, Lena Wong, and Matthew Kunofsky))
Public Health Research Institute, New York, NY 10016

Filamentous phages Ff(M13,fd,f1), IKe, and If1 have Class I protein coat structures on the basis of X-ray diffraction; I22 and X1 are in Class I on the basis of sequence. The DNAs in these viruses have anti-parallel strands of stacked bases, but not uniform pairing. One type of model for Class I has ten close-packed α-helical segments surrounding the DNA, five from each of two neighboring levels in the helix of subunits (1). Electrostatic theory for symmetry matching between DNA and protein helices shows that both 10- and 12-fold DNA helices can match Class I protein symmetry (2), and a recent proposal calls for 12-fold DNA in Ff (3).

Far UV CD spectra of Class I viruses are dominated by strong contributions from α-helices, along with huge tryptophyl contributions (4). Near UV tryptophyl CD contributions can be reduced by means of N-bromosuccinamide titrations, leaving CD spectra that look like those of base-stacked DNA, but with **negative** maxima at 276 nm. Previous CD results have shown that the DNA helices are **right-handed**. One interpretation of the apparent **negative** maxima at 276 nm for **right-handed** base-stacked DNAs, based on correlations of CD with helical twist, is that the DNAs in Class I viruses have about 10 bases per turn, not 12.

(1) L. Makowski & D.L.D. Caspar, *J. Mol. Biol.* **145** , 611 (1981); C.J. Marzec & L.A. Day, *Biophys. J.* **53** 425 (1988); (2) C.J. Marzec & L.A. Day, *Biophys. J.* **67** 2205 (1994); (3) G. Kishchenko & L. Makowski, *Biophys. J.* **70-2**, A363 (1996). (4) G.E. Arnold , L.A. Day, & A.K. Dunker, *Biochemistry* **31**, 7948 (1992).

Th-AM-I3

VISUALIZATION OF tRNAs IN THE *E. COLI* 70S RIBOSOME IN PRE- AND POST-TRANSLOCATIONAL STATES

((**Rajendra K. Agrawal**[1], Suman Srivastava[1], Ralph Jünemann[2], Niels Burkhardt[2], Pawel Penczek[1], Robert Grassucci[1], Knud H. Nierhaus[2], and Joachim Frank[1])) [1]Wadsworth Center, NY State Department of Health, Albany, New York, 12201-0509, U.S.A.; and [2]Institut für Molekulare Genetik, Max-Planck Institut, Berlin, Germany.

Knowledge of arrangements of mRNA and tRNAs in pre- and post-translocational states is crucial in understanding the mechanism of protein synthesis. Three-dimensional (3D) cryo-maps of the biologically active *Escherichia coli* 70S ribosome•mRNA•(tRNA)$_2$ complex have been obtained in both the defined states. First, the ribosomes were programmed with heteropolymeric mRNA and bound with corresponding tRNAs in ribosomal A- and P-sites in the pre-translocational state, and then were enzymatically translocated to P- and E-sites, in the post-translocational state. To localize the positions of tRNAs, difference maps were computed by subtracting the 3D cryo-map of naked ribosome from the 3D cryo-maps of pre- and post-translocational complexes. Results indicate that: (i) the relative arrangements of two tRNAs in pre- and post-translocational states are similar; and (ii) the tRNA•mRNA•tRNA complex moves toward the 50S subunit during translocation from pre- to post-state.

Th-AM-I4

DYNAMICS OF SINGLE tRNA AND RIBOSOMAL COMPLEXES UNDER PHYSIOLOGICAL CONDITIONS WITH TIME-RESOLVED SCANNING OPTICAL MICROSCOPY.

((Y. Jia, L. Li, S. Vladimirov, A. Sytnik, B. S. Cooperman, R. M. Hochstrasser)) Chemistry Department, University of Pennsylvania, Philadelphia, PA, 19104. (Spon. by C. M. Phillips)

Time-resolved *far-field* and *near-field* scanning optical microscopy have the potential to detect single molecules and provide *sub-nanosecond* resolution probes of numerous physical, chemical, and biological processes. The aforementioned techniques furnish unique opportunities to monitor protein biosynthesis in real time on the structural level of *single* ribosomal complexes. Toward this goal, we have labeled specific sites of tRNA with a single fluorescent probe. A labeled tRNA molecule and its complex with the ribosome have been observed with fluorescence imaging methods under conditions suitable for polypeptide chain growth. The fluorescence decay functions of single molecules of tetramethylrhodamine specifically bound to different sites of tRNA will be contrasted with fluorescence decays of the single probe molecules incorporated in a polymer film. Site specific dynamics is observed and will be discussed in the context of the tRNA and ribosome structure in the vicinity of the probe. Nonexponential behavior at the single molecule level has provided information about the structural equilibria in these systems.

Th-AM-I5

CONFORMATIONAL CHANGES INDUCED IN TELOMERIC DNA BY THE α SUBUNIT OF THE *Oxytricha nova* TELOMERE BINDING PROTEIN.

((**L. Laporte** and G. J. Thomas, Jr.)) Division of Cell Biology and Biophysics, School of Biological Sciences, University of Missouri, Kansas City, MO 64110.

Telomeres are DNA-protein complexes that stabilize the 3′ termini of eukaryotic chromosomes. The telomeric sequence of *Oxytricha nova*, d(T_4G_4)$_2$, interacts with a heterodimeric (α/β) telomere-binding protein both *in vivo* and *in vitro*. The α and β subunits are each able to form binary complexes with telomeric DNA as well as a ternary α:β:DNA complex. The adjoining 5′ DNA "tail" is known to affect binding of the β subunit [Fang et. al. (1993) *Biochemistry 32,* 11646]. We have investigated interactions between the α subunit and the telomere-containing sequences, d(T_4G_4)$_2$ and dT_6(T_4G_4)$_2$, using gel electrophoresis and Raman, fluorescence and CD spectroscopies. The results indicate that the α subunit binds to both d(T_4G_4)$_2$ and dT_6(T_4G_4)$_2$, but induces significantly different structural changes in the two DNA substrates, implying that the 5′ tail also plays a role in binding of the α subunit. Preliminary interpretation of the spectral data suggests that while both d(T_4G_4)$_2$ and dT_6(T_4G_4)$_2$ assume similar hairpin-like structures stabilized by G:G base pairs in the absence of α, their respective complexes differ in details of nucleoside and backbone conformation. The thymine tail of dT_6(T_4G_4)$_2$ is proposed as a participant in α-subunit recognition and may play a key structural role in the formation of the ternary complex. [Supported by NIH grant GM54378.]

Th-AM-I6

INTERPHASE CHROMOSOME BANDING: APPROACHING THE FUNCTIONAL ORGANIZATION OF THE HUMAN CHROMOSOME 15

((**Daniele Zink**[1], Harald Bornfleth[2], Astrid Visser[3], Christoph Cremer[2] and Thomas Cremer[1]))[1]Institut für Anthropologie und Humangenetik, LMU München, Richard-Wagner-Str. 10/I, D-80333 München, Germany, fax: ++49-89/5203-389; [2]Institut für angewandte Physik, Universität Heidelberg, Albert-Überle-Str. 3-5, D-69120 Heidelberg, Germany; [3]University of Amsterdam, Dept. of Radiobiology, Meibergdreef 9, 1105 AZ Amsterdam, The Netherlands

R-bands and G- or C-bands of human chromosomes were labeled specifically by incorporating two different thymidine analogs into the DNA during defined time segments in the S-phase. The distribution of the DNA assigned to the distinct chromosomal bands was investigated in the G_0- or G_1-stages of the interphase. The analysis focused on individual segregated chromosome 15 territories. The different chromosomal bands occupied distinct and essentially non-overlapping domains within the interphase territory. This result is in agreement with models that predict a close relationship between the structure of metaphase and interphase chromosomes. The chromosomal band domains were dynamically rearranged in G_1 compared to the quiescent state. Distinct types of chromosomal band domains were affected differently by the cell cycle dependent structural reorganization. The biological implications of these findings will be discussed

Th-AM-I7

REAL-TIME KINETIC ANALYSIS OF NUCLEASE-DNA BINDING AND CLEAVAGE ((JP Nolan[1], B Shen[2], MS Park[1], and LA Sklar[1,3])) Life Sciences Division[1], Los Alamos National Laboratory, Los Alamos NM 87545, Dept. of Tumor Biology[2], City of Hope National Medical Center, Duarte, CA 91010 and Cytometry[3], University of New Mexico, Albuquerque, NM, 87131

We have analyzed the mechanism of human flap endonuclease-1 (FEN-1) cleavage of its DNA substrate using a novel flow cytometric approach which provides sensitive and quantitative real-time kinetic data. By immobilizing either the DNA substrate or FEN-1 on a microsphere, we are able to measure continuously the kinetics of enzyme-substrate association, dissociation, and cleavage. When the flap DNA substrate is immobilized, substrate concentrations are low (~50 pM) allowing enzyme to be used in excess for single turnover kinetic studies. When FEN-1 is immobilized, the binding of fluorescently labeled DNA ligands can be measured directly. We have analyzed the cleavage reaction in terms of a simple two-step model consisting of a binding step followed by a cleavage step. This analysis indicates diffusion-limited binding of enzyme to substrate to form an enzyme-substrate (ES) complex (k_{on} = 1.1e^6/M*sec). The ES complex dissociates with a half-time of 10 seconds ($k_{off} \leq 0.07$/sec). When Mg^{2+} is added, cleavage of the ES complex occurs with a half-time of ~7 seconds ($k_{cleave} \leq 0.1$/sec). The kinetics of this Mg^{2+}-jump experiment are slower than expected, and both ES dissociation and cleavage kinetics are significantly faster when FEN-1 is immobilized and the smaller DNA is free to diffuse. These data are consistant with a mechanism in which E-S binding is followed by a conformational change which is sensitive to molecular size (such as sliding along the DNA strand) before strand cleavage occurs. Supported by RR01315.

Th-AM-I8

A CONTINUOUS TRAJECTORY OF DNA BENDING IS MADE POSSIBLE BY GRADUAL CHANGES IN THE TORSION ANGLE OF THE GLYCOSIDIC-BOND. ((Leonardo Pardo[1,2], **Nina Pastor**[1] and Harel Weinstein[1]))[1]Dept. of Physiology and Biophysics, Mount Sinai School of Medicine, New York, NY 10029, USA.[2]Lab. de Medicina Computacional, U. de Bioestadística, Fac. de Medicina, Universidad Autónoma de Barcelona, 08193 Bellaterra, Barcelona, Spain.

Structural comparisons have led to the suggestion that the change in the track of A-DNA required to form the TA-DNA conformation of DNA observed in the complex with the TATA-box binding protein (TBP), could be completed by modifying only the value of the glycosidic-bond χ by about 45°. The lack of a high number of crystal structures of this type makes it difficult to conclude whether the transition from A-DNA to TA-DNA can occur without disrupting either the Watson-Crick base pairing or the A-DNA conformation of the backbone. Molecular dynamics simulations of the dodecamer d(GGTATATAAAAC) demonstrate the feasibility of a continuous path in the A-DNA to TA-DNA transition and different extents of DNA curvature attainable with a χ angle value corresponding to B-DNA in the context of a backbone structure corresponding to A-DNA.

Supported by a grant from the Association for International Cancer Research, grants from DGICYT (PB95-0624 and PR95-275 to LP) and by a Fulbright/CONACyT (Mexico) scholarship (to NP).

Th-AM-I9

INITIATION OF TRANSCRIPTION BY T7 RNA POLYMERASE
((Craig T. Martin, Iaroslav Kuzmine, & Benjamin F. Weston))
Department of Chemistry, University of Massachusetts, Amherst, MA 01003-4510

In determining a unique site along the DNA for the initiation of transcription, an RNA polymerase must bind to upstream elements in the promoter DNA, and must direct the initial templating bases of the DNA (+1 and +2) precisely into the polymerase active site. However, after the initiation of transcription, the enzyme should behave as a sequence-independent polymerase, accommodating any templating bases into the active site. It is clear from previous studies, that one function of the upstream sequence "TATA" (-4 to -1) is to provide a low barrier to the melting of the DNA at the adjoining transcription start site, however, localized melting is not sufficient to uniquely define the start site. In order to characterize the role of this DNA in positioning the start site, we have incorporated into the promoter at unique positions, a variety of alkyl and polyethylene glycol spacers. A wide variety of spacers are accommodated with only slight effects on the kinetics of initiation, however, incorporation of even the most conservative of spacers leads to a significant decrease in start site fidelity. The results indicate that contacts upstream of position +1 play a role in the precise positioning of the start site, but that such positioning is not rate determining in the initiation of transcription.

Th-AM-I10

PRE-STEADY-STATE KINETIC STUDIES ON T 7 RNA POLYMERASE AND ITS MUTANT Y639F. ((**A-Y.M. Woody**, P.A. Osumi-Davis and R. W. Woody)) Department of Biochemistry and Molecular Biology, Colorado State University 80523-1870

Pre-steady-state kinetic measurements allow individual steps in the reaction pathway to be determined. The active-site mutants may display altered characteristics in the reaction steps from those of the wild-type. Pre-steady-state kinetic analysis of the addition of the single nucleotide to an initiating dinucleotide to form GpGpA on a 22 bp oligonucleotide template containing the T7 promoter gives biphasic reaction progress curves for the wild-type and the mutant Y639F. The data were fit to an exponential followed by a linear phase and analyzed by a non-linear least squares method. The normalized burst amplitudes were 0.3 and 0.06 for the wild-type and the mutant. From the rate constants for the addition step estimated from the initial rate constants at varying ATP concentrations , and from the burst amplitudes and the slopes of the linear phase obtained at 100 μM ATP, the rate constants for the reverse step of GGA formation and the release of GGA were estimated. The rate constants for the reverse step are quite significant and the value for the mutant is substantially larger than that of the wild-type. Future experiments will include pyrophosphate exchange reaction as well as pyrophosphorolysis. Our data will be discussed in the context of abortive initiation, the role of Tyr639, and the rate- determining step. Supported by NIH Grant GM23697 (A-YMW)

SPECTROSCOPIC STUDIES

Th-AM-J1

SINGLE CRYSTAL EPR STUDY OF THE Ni CENTER IN HYDROGENASE.
((C. Gessner, Y. Higuchi*, **W. Lubitz**)) Max-Volmer-Institut, Technische Universität Berlin, D-10623 Berlin, Germany; *Department of Chemistry, Graduate School of Science, Kyoto University, Kyoto 606-01, Japan.

Hydrogenases catalyze the reversible oxidation of molecular hydrogen. NiFe-hydrogenases contain a heterodinuclear Ni-Fe center, which is believed to form the active site of the enzyme. The three-dimensional structure of this enzyme from *Desulfovibrio gigas* and *D. vulgaris* was determined by X-ray crystallography (Volbeda et al. 1995, *Nature* **373**:580; Higuchi et al. 1994, *Acta Cryst.* D **50**:781), recently a resolution of 1.8 Å was achieved. The coordination of Ni and Fe is shown in the figure. The five ligands of Ni form a distorted octahedron, with one site left unoccupied. EPR measurements on single crystals of hydrogenase from *D. vulgaris* enabled us to determine the *g*-tensor of the paramagnetic Ni-site (S=1/2) in two different states of the oxidized enzyme, Ni-A and Ni-B (Gessner et al. 1996, *Chem. Phys. Lett.* **256**:518). Comparison of the results with the refined three-dimensional structure (Higuchi et al., unpublished) showed that the g_z-axis lies in the direction of the empty coordination site and parallel to one Ni–S bond, both in Ni-A and Ni-B. The directions of the g_x and g_y axes approximately coincide with the other metal–ligand bond directions in Ni-B (see figure), they are rotated by 25-30° in Ni-A. ENDOR experiments on single crystals of hydrogenase have also been performed to measure the proton hyperfine couplings of the ligands.

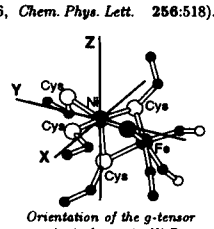

Orientation of the g-tensor principal axes in Ni-B.
○:*S*, ○:*O*, •:*C*, ●•:*not assigned.*

Supported by BMFT, Deutsche Forschungsgemeinschaft and the Ministry of Education, Science and Culture of Japan.

Th-AM-J2

RAMAN, INFRARED, AND TIME-RESOLVED FLUORESCENCE SPECTROSCOPIC STUDIES OF 2-AMINOPURINE AND OLIGONUCLEOTIDES. ((**K.O. Evans**, A. Kudryavtsev, D. Xu, and T.M. Nordlund)) University of Alabama-Birmingham, Birmingham, AL 35294

The DNA base analog 2-aminopurine (2AP) has been identified as a highly fluorescent molecular probe of DNA that is a thousand times more fluorescent than its sister molecule adenine. When incorporated into the decamer d[CTGA(2AP)TTCAG]$_2$, 2AP was found to possess multiple fluorescence decay components, suggesting that 2AP exists in multiple conformations. [1] To determine the nature of the conformations, we performed 2D NMR experiments on 2AP deoxy- and ribonucleoside, which showed in DMSO comparable amounts of *syn* and *anti* conformations. However, neither time-resolved fluorescence nor fluorescence spectral analysis [2,3] showed evidence of multiple components. Thus, the presence of *syn* and *anti* conformations in a nucleoside monomer is not, by itself, sufficient enough to cause multi-exponential decay. Also, we will present the effects of dinucleoside stacking, temperature, and nearest neighbor on the Raman and infrared spectra of 2AP.

[1] P. Wu, H. Li, T.M. Nordlund, and R. Rigler (1990) *Proc. SPIE* **1204**, 262-269.
[2] K.O. Evans, D. Xu, Y. Kim, and T.M. Nordlund (1992) *J. Fluorescence* **2**, 209-216.
[3] D. Xu, K.O. Evans, and T.M. Nordlund (1994) *Biochemistry* **33**, 9592-9599.
Supported in part by NSF grant MCB-9118185 and ONR N00014-94-1-1023.

Th-AM-J3

QUANTUM MECHANICAL - MOLECULAR DYNAMICS SIMULATION OF TRYPTOPHAN FLUORESCENCE IN PROTEINS. ((B.K. Burgess and **P.R. Callis**)) Dept. of Chemistry and Biochemistry, Montana State University, Bozeman, MT 59717.

We have extended our hybrid QM-MD method for predicting the fluorescence wavelength of an indole in water [P. Muino and P. Callis,(1994) J. Chem. Phys. *100*, 4093] to tryptophans in proteins. All-atom dynamics using Discover was applied to protein structures derived from 17 protein crystal structures. The electrostatic potential and electric field at the tryptophan (trp) ring atoms was computed from the atomic charges provided by the CVFF force field and included in the Fock hamiltonian of an INDO/S-CI calculation applied to a 3-methylindole molecule with standard geometry. The trp of interest is solvated with a 10-15 Å layer of water, to the extent allowed by the protein environment. At present, the predicted wavelength is based on the average transition energy 0.4-1.0 ps following simulated excitation. Of 23 trps simulated, representing a range of exposure to solvent, 17 are predicted within 7 nm of the experimental value. Buried trps show no significant relaxation during this time period and exhibit only small amplitude fluctuations; partially exposed trps show a large relaxation (time-dependent red shift), which correlates with the number of nearby waters, and larger fluctutations. The fluctuation amplitude correlates with diffuseness of the observed spectra. The method promises to be useful in testing theories of electrostatics in proteins.

Th-AM-J4

DATABASE OF EXPERIMENTALLY INTERESTING PROTEINS FOR FLUORESCENCE STUDIES. ((**CHRISTOPHER HOGUE**)) NCBI, NLM, NIH. 8600 Rockville Pike, Bethesda MD 20894.

A database service to satisfy the kinds of queries made by biological fluorescence spectroscopists is described. The database is a set of hypertext documents built using the Entrez integrated sequence/structure/reference database system. The Entrez database is optimized for a particular subset of queries, such as keyword searching, or queries based on similarity scores. Some database queries are not well-supported by the Entrez indexing scheme, deemed "rare, detailed queries". One query commonly asked by fluorescence spectroscopists is: "Give me a list of proteins with a single Trp." This is based on a desire to find experimentally valuable proteins. As the intrinsic fluorescence signal from Trp in proteins has a very broad bandpass, the most interesting systems are those which provide a fluorescence signal from a single Trp. This intrinsic reporter can help identify and localize conformational changes, protein interactions, refolding events, and information about protein dynamics. To satisfy the query, one must construct a program that counts Trp residues in each sequence in the database. Further query refinements often take the form: "Single Trp proteins which are like a known sequence or structure", or "Single Trp proteins taken from a complete genome of some organism". Two autonomous agent programs, TRPSTRU, and TRPORG have been constructed to implement these queries and to provide their results in the form of HTML tables which are updated regularly. TRPSTRU provides a list of single-Trp and Trp-free protein structures derived from MMDB, the 3-D structure division of Entrez which is based on the PDB database. In addition TRPSTRU provides lists of single-Trp and Trp-free proteins which are similar to known structures. TRPORG finds single-Trp and Trp-free sequences from a variety of complete genomes, from which scientists may obtain DNA for constructing expression systems. TRPORG also finds similar sequences to these genomic proteins that are single-Trp and Trp-free. See the Biophysical Society Fluorescence Subgroup page for WWW access to this database: `http://biosci.cbs.umn.edu/biophys/subgroup.html`.

Th-AM-J5

CHARACTERIZATION OF FLUORESCENCE QUENCHING IN BICHROMOPHORIC PROTEASE SUBSTRATES. ((**Beverly Z. Packard**, Dmitri D. Toptygin, Akira Komoriya, and Ludwig Brand)) OncoImmunin, Inc., College Park, MD and Johns Hopkins University, Baltimore, MD

A series of relatively rigid, bent polypeptides each of which contains an amino acid sequence that is recognized by a specific protease has been designed and synthesized. Covalently labeling substrates with a flurophore on each side of their cleavage sites enables one to use a change in fluorescence intensity as a measure of enzymatic activity. In this study we have used the cleavability of doubly-labeled substrates as a tool to examine intramolecular resonance dipole-dipole interactions. Specifically, we have made both homo- and hetero bichromophoric substrates and measured their absorption and fluorescence properties in order to contrast the Förster model of resonance energy transfer with the exciton model of delocalized excitation. The latter is of interest since both types of labeled intact peptides exhibit blue-shifted absorption maxima and quenched fluorescence; these spectral elements are ascribed to formation of intramolecular ground-state complexes between fluorophores and can be described by exciton theory. Spectral properties of the two types of doubly-labeled substrates were further characterized using singly-labeled peptides as well as the chaotropic agent urea. Additionally, a comparison of fluorophores, e.g., xanthenes, coumarins, and pyrene, was made in terms of their ability to form intramolecular dye-dye dimers. (Supported in part by NIH grant GM11632.)

Th-AM-J6

FLUORESCENCE LIFETIME-BASED DETERMINATION OF CYANIDE USING A CARBONIC ANHYDRASE-BASED BIOSENSOR

((**R.B. Thompson***, H.J. Lin, Z. Ge, K. Johnson#, and C.A. Fierke#)) Dept. Biochem. Mol. Biol., Univ. Maryland Med. School, 108 N. Greene St., Baltimore, MD 21201; and #Dept. Biochem., Box 3711, Duke Univ. Med. Center, Durham, NC 27710.

Small anions such as cyanide, nitrate, bicarbonate, azide, cyanate, and others are analytically of substantial importance. While methods exist for determining these anions in discrete samples, there are few good techniques for monitoring their levels continuously, particularly in complex media such as serum or sea water. We have heretofore exploited the high selectivity of the metalloenzyme carbonic anhydrase for certain divalent cations such as zinc to develop fluorescence-based metal ion biosensors of high sensitivity (1-3). It is well known that carbonic anhydrase is inhibited to varying degrees by several different anions, which typically bind as a fourth ligand to the active site Zn(II). When the Zn(II) is replaced by Co(II), these anions continue to bind, but can significantly perturb the weak d-d absorbance of the bound Co(II). For a suitable fluorophore covalently attached close to the metal, this perturbation results in an altered efficiency of fluorescence resonance energy transfer, which can be observed by measuring the time dependence of the fluorescence in the frequency domain. Thus by using a CY-3-labeled N67C site-directed mutant of human carbonic anhydrase II, we can determine the concentration of cyanide and cyanate by measuring the change in phase angle and modulation of the fluorescent label as the anion is added.

(1) *Anal. Chem.* 65, 730-734 (1993); (2) *Anal. Biochem* 227, 123-8 (1995); (3) *Biosens. Bioelect.* 11, 557-564 (1996).

Sponsored by the Office of Naval Research and the National Science Foundation.

Th-AM-J7

Multiphoton-Excited Photochemistry Yields Visible Emission From Serotonin. **((Jason B. Shear*, Chris Xu, and Watt W. Webb)) Applied Physics, Cornell University, Ithaca, NY 14853**

Nonlinear excitation of neurotransmitter serotonin (5HT) in aqueous solution is shown to generate a blue-green emitting photoproduct in addition to UV fluorescence characteristic of native 5HT. The visible emission rate in diffusional steady-state measurements scales as the sixth-power of excitation intensity, demonstrating that absorption of six near-IR photons is required for emission of one visible photon. Transient measurements reveal that this process is composed of two sequential nonlinear steps, the first excited by four photons and the second by two photons. These results, in combination with measurements of three-photon-excited serotonin UV fluorescence and four-photon bleaching support a model in which 5HT is photochemically transformed as a consequence of four-photon absorption (E_{tot} = 6 eV) to a photoproduct that then emits in the visible region via two-photon excitation. A minimum bound of ~10^{-51} cm^4 s/photon is observed for the two-photon emission action cross section of the photoproduct at 830 nm. Photoionization, rather than reaction with a dissolved oxygen species, appears to be the primary mechanism for generation of the blue-green emitting photoproduct. The intensities required to generate significant blue-green photoproduct are approximately tenfold higher than are typically used in two-photon laser scanning microscopy, but are still one order of magnitude lower than the estimated intensity needed to induce dielectric breakdown of water.

*Present address, department of chemistry, University of Texas, Austin, TX 78712.

Supported by the Developmental Resource for Biophysical Imaging and Opto-electronics funded by NSF(DIR8800278), NIH(RR04224) and NIH(RR07719). J. S. was an NSF Postdoctoral Fellow supported by Grant CHE-9403174.

Th-AM-J8

IDENTIFICATION OF THE PRINCIPLE SOURCES OF TWO-PHOTON AUTOFLUORESCENCE FROM HeLa CELL MONOLAYERS. ((**M.G. Nichols**[1], J.A. Nichols[2], and W.W. Webb[1])) Departments of [1]Applied and Engineering Physics and [2]Chemistry, Cornell University, Ithaca, NY 14853.

Quantitative imaging of endogenous fluorophores such as reduced pyridine nucleotides (NAD(P)H) and oxidized flavins can provide information regarding the status of cellular metabolism as well as details of the local microenvironment. To identify the chemical species and quantify their respective contributions to the total autofluorescence signal, two-photon fluorescence images (emission from 400-520 nm) of HeLa cell monolayers were obtained at excitation wavelengths ranging from 700-805 nm delivered by a mode-locked Ti:sapphire laser. A comparison with the two-photon cross section spectra of biologically relevant fluorophores[1] indicates that NAD(P)H is the primary source of the HeLa cell autofluorescence signal in this wavelength range. We are currently in the process of extending the excitation spectrum to 1000 nm, where flavin emission is expected. We are also attempting to measure the autofluorescence emission spectrum with sufficient spatial resolution to discriminate between mitochondrial and cytoplasmic signals. Since the pyridine nucleotide redox state is coupled to the local oxygen concentration, changes in the tumor cell fluorescence is being explored to provide a much needed non-invasive diagnostic indicator of anoxia in tumors. Because development of anoxia can severely undermine the efficacy of cancer therapies, such as photodynamic therapy (PDT), which function by producing cytotoxic oxygen species from molecular oxygen, we are applying this approach to monitor multicell tumor spheroids during PDT.

[1] Xu *et al.*, Proc. Natl. Acad. Sci. USA 93:10763-10768, 1996.

Supported at DRBIO by the NIH (RR04224 and RR07719) and NSF (BIR 9419978). M.G.N. is an NIH Postdoctoral Fellow supported by NRSA 1 F32 CA 72225-01.

Th-AM-J9

TIME-RESOLVED SPECTROSCOPY OF WILD-TYPE AND MUTANT GREEN FLUORESCENT PROTEINS

((H. Lossau[§], A. Kummer[§], F. Pöllinger-Dammer[§], C. Kompa[§], T. Jonsson[†], C.M. Silva[†], M.M. Yang[†], D. Youvan[†] and M.E. Michel-Beyerle[§]))
[§] Institut für Physikalische und Theoretische Chemie, TU München, D-85748 Garching, Germany
[†] KAIROS Scientific Inc., 3350 Scott Blvd., Bldg. 62, Santa Clara, CA 95054

In the light of the recent X-ray structure of wild-type Green Fluorescent Protein (GFP) [1] its excited state dynamics has been investigated with special emphasis on mutations which lead either to mechanistic insight or to striking changes of the emission properties, a goal at the heart of biotechnology. The key process underlying emission phenomena of wild-type GFP is excited state deprotonation. This process is shown to follow highly dispersive kinetics with respect to both, the spread in time constants and emission wavelengths covering a spectral range from 400 nm to 700 nm. The temporal evolution of dispersive deprotonation has been investigated in the temperature range 300 K - 80 K using picosecond time-resolved fluorescence measurements, complemented by femtosecond transient absorption spectroscopy. Lowering the temperature to 80 K shows that the dispersive kinetics is only slightly activated in wild-type and deuterated GFP, the latter one deprotonating at all temperatures on a longer time scale. Along this line of ultrafast spectroscopy the effects of external parameters as pH, ionic strengths and hydrophilic/hydrophobic nature of solvent will be presented and related to protein dynamics.

[1] F. Yang, L.G. Moss and G.N. Phillips, Nature Biotechnology, 14, 1246-1251
D. Youvan and M.E. Michel-Beyerle, Nature Biotechnology, 14, 1219-1220

Th-AM-J10

ETIOLOGY AND GROWTH FACTORS IN BRAIN ANEURYSMS

(G.Austin, B.Blackbourne, S.Fisher, R.Gaskell, W.Schievink)
The Stroke Research Foundation, UCSB, Santa Barbara, CA 93106

Brain Aneurysms (BA) are present in 8% of the population at consecutive autopsies for all causes. They vary in size from 2mm to 75mm in diameter. Most commonly they arise from branching arteries of the internal carotid, middle cerebral, or anterial communicating vessels. None are congenital. According to Schievink et. al. in a series of 133 consecutive brain aneurysms discovered serendipitously at the Mayo Clinic, no BA smaller than 10mm in diameter ruptured over an 8.2 year follow-up period and the average diameter at rupture was 22mm. There are strong genetic factors in their formation. In adult polycystic kidney disease, APKD, the most common of all genetic defects, 20% also had BA. Although no clear cut cause of rupture is known, wall thickness is important and the average thickness at rupture was 30 microns of collagen. Immuno-fluorescent studies in our BA research lab at UCSB show that there is loss of the normal 3-layered arterial architecture in BA so that their walls are composed essentially of an IEM and a single blended media and adventia layer composed of Collagen Type I and fibronectin.

MITOCHONDRIAL CHANNELS

Th-AM-K1

FUNCTIONAL DIFFERENCE IN YEAST-EXPRESSED WHEAT VDAC ISOFORMS

((A. Elkeles*, A. Breiman* and M. Zizi#))*Tel Aviv Univ., Israel, #K.U.Leuven, Belgium.

The mitochondrial outer membrane (OM) contains a pore protein that forms voltage-dependent anion-selective channels (VDAC) in reconstituted systems. By regulating the flow of AT(D)P and metabolites across the OM, the gating of the channel -which is a monomer- presumably controls mitochondrial metabolism. Regardless of their origin, VDAC channels cannot be easily distinguished, here we are reporting functional differences between VDAC isoforms *in vivo* and *in vitro*. 3 VDAC cDNAs cloned from wheat were successfully expressed in a *vdac*-minus yeast strain unable to grow on glycerol as sole carbon source. Growth phenotypes and channel function were monitored. Cells expressing *Tavdac1* and *Tavdac2* had growth curves superimposable to the control yeast. *Tavdac3* expression however consistently resulted in a 50% decrease in doubling time during the logarithmic growth phase while reaching a similar growth maximum. In planar membranes, the 3 purified isoforms yielded voltage-dependent anion selective channels with electrophysiological parameters (single channel conductance, ion selectivity and gating) comparable to known VDACs. Features unique to the wheat channels are however reported. The isoforms display specific -preferred- conductance levels, kinetics and current rectification easily differentiating them. Use of protease inhibitors during protein purification of wheat and yeast isoforms, and addition of pronase on reconstituted channels, allowed us to ascertain that some of the unique wheat VDAC channel properties resulted from co-purification of a channel-modulating protein. The latter is functionally different from the VDAC modulator. While strenghtening VDAC role in metabolism, our results indicate that VDAC functional diversity may usually be lost by purification procedures. Our results are consistent with VDAC functioning as a heteromer including one pore protein and other modulating subunits. (Grants: JSM-RT G96/02, NFWO 271111 to MZ, GIF to AB).

Th-AM-K2

IDENTIFICATION OF A SECOND YEAST VDAC GENE

[(E. Blachly-Dyson*, J. Song#, M. Colombini# and M. Forte*) *Vollum Institute, Oregon Health Sciences University, Portland, OR 97201; # Dept. of Zoology, University of Maryland, College Park, MD 20742. (Spon. by M. Forte)]

The permeability of the outer mitochondrial membrane to most metabolites is believed to be based in an outer membrane protein forming a voltage-dependent anion channel (VDAC). The yeast, *Saccharomyces cerevisiae*, has been thought to contain a single VDAC gene, designated *POR1*. However, cells missing the *POR1* gene (*Δpor1*) were able to grow on yeast media containing a non-fermentable carbon source although not on such media at elevated temperature (37°C). If VDAC normally provides the pathway for metabolites to pass through the outer membrane, some other protein(s) must be able to partially substitute for that function. In order to identify proteins that could functionally substitute for *POR1*, we have screened a yeast genomic library for genes which, when overexpressed, can correct the growth defect of *Δpor1* yeast grown on glycerol at 37°C. This screen identified a second yeast VDAC gene, *POR2*, encoding a protein (YVDAC2) with 49% amino acid sequence identity to the previously identified yeast VDAC protein (YVDAC1). YVDAC2 can functionally complement defects present in *Δpor1* strains only when it is overexpressed. Deletion of the *POR2* gene alone had no detectable phenotype, while yeast with deletions of both the *POR1* and *POR2* genes were viable and able to grow on glycerol at 30°C, albeit more slowly than *Δpor1* single mutants. Subcellular fractionation indicates that YVDAC2 is normally present in the outer mitochondrial membrane. Finally, mitochondrial membranes made from wild-type cells, *Δpor1* cells, *Δpor1, Δpor2* cells and *Δpor1* cells overexpressing YVDAC2 were incorporated into liposomes and the permeability of resulting liposomes to non-electrolytes of different sizes was determined. The results indicate that YVDAC2 does not confer any additional permeability to these liposomes, suggesting that it may not normally form a channel.

Th-AM-K3

PROBING THE PERMEABILITY OF THE MITOCHONDRIAL OUTER MEMBRANE BY MEASURING THE NADH OXIDATION RATE OF YEAST MITOCHONDRIA EXPRESSING DIFFERENT VDAC GENES

((A. Lee*, X. Xu*, E. Blachly-Dyson#, M. Forte# and M. Colombini*)) *Dept. of Zool., Univ. of Maryland, College Park, MD20742; #Vollum Inst., Oregon Health Sciences Univ., Portland, OR 97201.

The metabolite flux between the cytosol and the mitochondrial spaces is essential to mitochondrial function. Often the mitochondrial outer membrane is assumed to be highly permeable and not rate limiting. Recent reports indicate that changing the outer membrane permeability by changing the state of VDAC results in changes in the rates of mitochondrial function. Agents that increase the voltage-dependence of VDAC channels in planar membranes also have consistent effects on mitochondrial respiration, by greatly inhibiting the flux of metabolites through the outer membrane. To study the roles of different VDAC genes in the control of outer membrane permeability, a new method was developed to convert the rate of NADH oxidation by an intermembrane space NADH dehydrogenase to an estimate of the outer membrane permeability to NADH. We found that yeast mitochondria missing YVDAC1 had a 20 fold reduction in permeability compared to wild-type mitochondria, while those missing both YVDAC1 and YVDAC2 have virtually the same properties as those missing only YVDAC1. Cells expressing only YVDAC2 have a slightly higher permeability than those expressing no VDAC at all. This indicates that YVDAC1 is the major pathway for NADH flux across the outer membrane in wild-type mitochondria and YVDAC2 has a minimal role in this permeability. (Supported by NIH grant GM35759)

Th-AM-K4

TOPOLOGY OF VDAC IN THE MITOCHONDRIAL OUTER MEMBRANE.

((Scott T. Stanley and Carmen A. Mannella)) Wadsworth Center, Empire State Plaza, Box 509, Albany, NY 12201-0509; Department of Biomedical Sciences, University at Albany, SUNY.

The topology of the VDAC protein in the outer membrane of mitochondria isolated from *Neurospora crassa* is being determined using antipeptide antibodies and partial proteolysis. Accessibility of epitopes on either side of the outer membrane is determined by antibody binding to mitochondria with intact or lysed outer membranes in suspension. Results indicate that epitopes in segments 129-145 and 251-268 are exposed to the cytosol, those in segments 1-20, 195-210, and 272-283 are exposed on the interior, and those in segment 60-76 are inaccessible to the aqueous phase. Locations of epitopes in each segment are being defined by determining whether preincubation of antibodies with N- or C-terminal halves of the immunizing peptides inhibits antibody binding to mitochondria. Partial proteolysis of mitochondria is performed with continuous monitoring of outer membrane integrity, using the battery of antibodies as probes for western blotting. Results with endo-GluC, trypsin, chymotrypsin, and ArgC indicate numerous cleavage sites on the cytosolic surface in regions 20-60, 80-100, 110-130, 145-180, and 190-230. In almost all cases, inferred cleavage sites occur in between the eleven segments in the VDAC polypeptide identified as possible transmembrane beta-strands by the Gibbs sampler (Mannella et al., 1996, J. Bioenerg. Biomembr. 28:163). This experimental data is being used to generate a folding model for the integral membrane form of fungal VDAC. (Supported by NSF Grant MCB-9506113.)

Th-AM-K5

Mitochondrial and Extra-Mitochondrial Human Porin are Identical

((Ulrike Stadtmüller[1], Angela Schmid[2], Roland Benz[2], Friedrich P. Thinnes[1] & Norbert Hilschmann[1])) [1]Max-Planck-Institut f. Experimentelle Medizin, D-37075 Göttingen, [2]Lehrstuhl für Biotechnologie, Universität Würzburg, D-97074 Würzburg, Germany (Spon. By C.A. Mannella).

In mammalian cells porin channels are localized in mitochondrial outer membranes as well as in the plasmalemma (Reymann, S. et al., Biochem. Mol. Med. 54, 75-87, 1995). Structure and function of these membranes are highly different, suggesting that they may harbour different types of porin which reflect two or more genes for eukaryotic porins in the genome. We isolated mitochondria-derived porin from a human B-lymphocyte cell line, determined its amino acid sequence and characterized its channel properties. Interestingly, the amino acid sequence elaborated from this porin preparation and correspondingly its electrophysiological characteristics in a reconstituting system were identical to those of „Porin 31HL", the human Type-1 porin which was purified from a crude membrane preparation of the same cell line but in a totally different way. These results raise important questions concerning targeting, insertion and orientation of human Type-1 porin in different membranes which will be discussed.

Th-AM-K6

INTERACTIONS OF THE MITOCHONDRIAL OUTER MEMBRANE WITH THE INNER MEMBRANE AND ENDOPLASMIC RETICULUM.

((C.A. Mannella, M. Marko, K. Buttle, D. D'Arcangelis, K. O'Farrell, K. Tessitore)) Wadsworth Center, Empire State Plaza, Albany, NY 12201-0509

Electron microscopic tomography is being used to determine the topology of mitochondrial membranes and their interactions with other cellular components. In isolated *condensed* (matrix contracted) rat-liver mitochondria, the cristae are large, pleiomorphic compartments connected to each other and to the surface of the inner membrane by narrow tubular regions. Individual cristae often have multiple small openings at the inner membrane. In *orthodox* (matrix expanded) mitochondria, intracristal compartments are flattened and less interconnected. Contacts between the inner and outer membranes typically occur as discrete domains 20-40 nm wide, with a surface density of several hundred per μm^2. Intermembrane contacts often flank sites at which the inner membrane folds inward to form cristae, suggesting possible involvement of contact-site components in inner-membrane invagination. A reconstruction has recently been completed of an in-situ rat-liver mitochondrion surrounded by endoplasmic reticulum. Numerous short extensions, spaced about 50 nm apart, protrude from the ER surface and make contact with the outer membrane in several different regions along the mitochondrial periphery. (Supported by NSF grants MCB-9506113, BIR-9322134, and NIH grant RR01219.)

Th-AM-K7

A HIGH-CONDUCTANCE CHANNEL, MCC, IS ASSOCIATED WITH TIM23, A COMPONENT OF THE PROTEIN IMPORT COMPLEX IN THE MITOCHONDRIAL INNER MEMBRANE

((T.A. Lohret[1], R.E. Jensen[2], A. Moodie[1], P.M. Sokolove[3], M.L. Campo[4] and **K.W. Kinnally**[1])) [1]Div. Molec. Med., Wadsworth Center, Albany, NY, [2]Dept. Cell Biol., Johns Hopkins Univ. Sch. of Medicine, Baltimore, MD, [3]Dept. Exp. Pharm. and Exp. Ther., Univ. of Maryland Sch. of Med., Baltimore, MD, [4]Dpto. de Bioquímica, Univ. de Extremadura, Spain.

We previously showed that peptides corresponding to mitochondrial import signals induce a rapid flickering of a mitochondrial inner membrane channel, called MCC. Several more peptides have been examined for their effect on yeast MCC reconstitued in proteoliposomes and for their ability to induce a permeability transition in isolated rat mitochondria. To determine if MCC plays a role in protein import, we examined this activity in a yeast strain defective in the import component, Tim23. In contrast to wild-type MCC, we find that the conductance of MCC from this import deficient mutant is not blocked by mitochondrial presequence peptides. Furthermore, we find that antibodies to Tim23 inhibit MCC activity at concentrations shown to inhibit mitochondrial protein import. In addition, the outer membrane peptide sensitive channel (PSC) activity is distinct from MCC since PSC is not affected by either a mutation in Tim23 or antibodies raised against Tim23. Our results show that Tim23 is required for normal MCC activity and raise the exciting possibility that precursors are translocated across the inner membrane through the channel MCC. Supported by NSF MCB 9513439, DGICYT PB95-0456.

Th-AM-K8

DNA CAN BE TRANSLOCATED ACROSS PLANAR BILAYER MEMBRANES CONTAINING MITOCHONDRIAL PORIN

((G.Bàthori, **I.Szabò**, F.Tombola, M.Brini, A.Coppola, M.Zoratti and V.DePinto[1])) CNR, CS Biomembranes, Dept. Biomedical Sciences, Padova, and [1]Inst. Biochem. Pharmaceutical Sciences, Catania, Italy (Spons. by M.Zoratti)

We are studying the translocation of DNA across membranes using a reconstituted system in which membrane vesicles or pore-forming proteins are incorporated into the planar bilayer of a BLM setup, and DNA is added to one of the chambers. Transport is detected using PCR amplification and Southern blotting. We report that when the bilayer contains purified mitochondrial porin (VDAC), DNA added in the cis chamber can be translocated to the trans side if a cis-side-negative potential is applied. No translocation takes place if: 1) no protein is incorporated, 2) the membrane contains Gramicidin A or 3) a 30 pS (100 mM KCl) anion-selective channel, and if 4) anti-VDAC antiserum is added after porin incorporation. The results support the idea that DNA translocation may be mediated by pores, and point to possible pathways of DNA entry (efflux) into (from) cells and mitochondria. (Supported by Telethon - Italy)

Th-AM-K9

MECHANISM OF MITOCHONDRIAL PERMEABILITY TRANSITION PORE INDUCTION BY N-ETHYLMALEIMIDE

((**P.Costantini**, R. Colonna and P. Bernardi)), CNR and Department of Biomedical Sciences, University of Padova, Via Trieste 75, I-35121 Padova, Italy (Spon. by C. Mannella).

We have investigated the mechanism by which high concentrations (≥0.5 mM) of N-ethylmaleimide (NEM) open the mitochondrial permeability transition pore (MTP), a voltage-dependent channel sensitive to cyclosporin A. We show that, following the uptake of Ca^{2+}, addition of NEM causes opening of the MTP after a short lag phase. Similar results could be obtained with the SH reagents mersalyl and methylmethanethiosulphonate (MMTS). Pore opening by NEM, mersalyl and MMTS was fully reverted by both dithiothreitol (DTT) and β-mercaptoethanol. Since reaction of NEM with SH groups in not reversed by DTT, we conclude that NEM causes the unmasking of a previously unrecognized redox-sensitive site and that the mechanism of pore induction by NEM involves the oxidation of this site. NEM, mersalyl and MMTS do not affect the resting membrane potential or its response to uncoupler in the presence of cyclosporin A, suggesting that they all cause a shift of the voltage threshold to more negative values, with MTP opening at physiological membrane potentials. We have previously demonstrated that the MTP is modulated by the redox state of two different sites: the P site, in apparent oxidation-reduction equilibrium with the pyridine nucleotide pool, and the S site, an oxidation-reduction sensitive dithiol in equilibrium with the glutathione pool. The site described here can be clearly discriminated from both the P and S sites, since the latter are completely blocked by 20 μM NEM.